# DESIGN OF MICROWAVE SINTERING UNIT FOR DEVELOPMENT OF COPPER-CHROMIUM CONTACT MATERIALS

*Thesis submitted in partial fulfilment of the requirements for the award of degree of*

**Master of Technology**

in

**Materials and Metallurgical Engineering**

*Submitted By*

**Mukul Verma**

**(Roll No. 600902007)**

Under the supervision of:

**Dr. O. P. Pandey**
Professor & Head
School of Physics and Materials Science
Thapar University
Patiala

**Dr. Janamejay Nemade**
Senior Manager-Technology
Global R&D Centre
Crompton Greaves Limited
Mumbai

SCHOOL OF PHYSICS AND MATERIALS SCIENCE

THAPAR UNIVERSITY

PATIALA-147004

**JULY 2011**

# Certificate

I hereby certify that the work which is being presented in the thesis entitled, "*Design of Microwave Sintering Unit For Development of Copper-Chromium Contact Materials*", in partial fulfillment of the requirements for the award of degree of Master of Technology in *Materials and Metallurgical Engineering* submitted in School of Physics and Materials Science of Thapar University, Patiala, is an authentic record of my own work carried out under the supervision of *Dr. O. P. Pandey and Dr. Janamejay Nemade* and refers other researcher's work which are duly listed in the reference section.

The matter presented in the thesis has not been submitted for award of any other degree of this or any other University.

Signature: Mukul Verma

(Mukul Verma)

This is to certify that the above statement made by the candidate is correct and true to the best of my knowledge.

**(Dr. O. P. Pandey)**
Professor & Head
School of Physics and Materials Science
Thapar University
Patiala

**(Dr. Janamejay Nemade)**
Senior Manager-Technology
Global R&D Centre
Crompton Greaves Limited
Mumbai

**Countersigned by:**

**(Dr. S. K. Mohapatra)**
Dean (Academic Affairs)
Thapar University
Patiala

# Acknowledgements

I would like to express my deep gratitude to all who contributed in successful conclusion of this work and submission of this dissertation.

I take this opportunity to express my deep sense of respect and gratitude to my thesis supervisors Dr. O. P. Pandey and Dr. J. B. Nemade who have suggested the problem for my dissertation and initiated me in the field of microwave sintering. I am indebted to them for their constant suggestions, encouragement, valuable guidance and cooperation without which this presentation would not have reached the present shape. Their guidance was immeasurable help to me in pursuing an industrially significant area for my M.Tech thesis desertation.

I express my immense gratitude and indebtedness to Mr. T. Rakesh, Mr. Sushil Jena, Dr. Dawid De'melo, Dr. Pradeep Roy, Dr. Asha Ingle of Advance Materials and Process Technology Centre, Crompton Greaves Global R&D for their continuous help and valuable suggestions throughout my M. Tech. program.

The technical support by Mr. P. Sarma, Mr. Sathya, Mr. Lokesh Chaudhary and Mr. Subhendhu Bhattacharya is thankfully acknowledged.

My sincere thanks are due to Mr. Vilas Lokhande and Mr. Basit Shaik for necessary help during my experimental work.

I would like to extend my sincere thanks to all my friends, who offered help patiently throughout the project.

Finally, I would like to share this moment of happiness with my parents and brother. The help of my family through all that has happened during my M. Tech. was astounding.

Mukul Verma

Thapar University, Patiala

June 2011

# Abstract

In the present work design modification and development of microwave sintering unit has been carried, to make it suitable for its usage at high vacuum, using traditional methodology which is assisted by modern analytical tool. The present work investigates the possibility of consolidating 75Cu-25Cr alloy through microwave sintering technique. An attempt has been made to compare the results of microwave sintered specimens with its conventional counterparts. This study also compares the sintering behaviour of 75Cu-25Cr alloy powder made with mechanical milled Cr powder in both conventional method as well as microwave method. The study also aims to understand the effect of mechanical milling on the sinterability and on different properties of same alloy developed in both conventional and microwave furnace. The phase evolution and morphological changes of the milled samples were carried out using X-ray diffraction (XRD) and scanning electron microscopy (SEM). The consolidation of green compacts was carried out at 1050 ºC with variation of sintering as a function of three peak soaking periods i.e. 30 minutes, 60 minutes and 180 minutes, and also with variation of three relative green density values i.e. 57% , 67% and 78% of theoretical density. The comparative analysis is based on the sintered density, hardness, electrical conductivity and microstructures of samples. The results show that microwave sintering requires about 75% less processing time as compared to conventional sintering for this alloy. The microwave sintered specimens showed superior mechanical properties compared to conventionally sintered counterparts due to better densification. Also, microwave sintered specimens have showed good enhancement in electrical conductivity. Microstructural study revealed that microwave sintering produces well rounded and finer chromium particles which are wellseparated from each other as opposed to the sharp, irregular and wedge shaped chromium particles for the conventionally-sintered samples. Also, microwave sintering resulted in significantly lower Cr grain coarsening.

# Contents

# List of Figures

# List of Tables

# Chapter 1 Introduction

Contact materials are two phase composite systems having 25 to 50% (wt. %) of refractory metals such as tungsten, molybdenum, WC and chromium as one phase and the balance is generally an electrically conducting material such as copper and silver. Out of these combinations, Cu-Cr alloys have been widely accepted and adopted for medium-voltage, high-current Vacuum Circuit Breakers (VCB).

A typical solid phase sintered microstructure of these alloys contains chromium (b.c.c) grains interspersed in ductile copper (f.c.c) matrix. The Cu-Cr alloys offer a unique combination of properties such as better current interrupting behaviour on load and overload conditions, low erosion losses on a high number of switching operations, low chopping currents, and good current carrying capacity. These properties make them potential candidate for electrical contact materials. The Cr plays an important role both in strengthening and in restricting grains coarsening of Cu matrix [1]. Because of refractoriness of chromium ($T_m$=1907°C) and negligible inter solubility between chromium and copper, Cu-Cr alloys are processed by powder metallurgical (P/M) route. The liquid phase sintered or infiltrated Cu-Cr alloys have more than half share of VCB market [2].

Microwave energy has emerged as the most versatile form of energy applicable in numerous diverse fields. Since its first use for radar in WWII, it is now being applied in communication, chemistry, rubber vulcanisation, drying, food processing, medical treatment and diagnosis and variety of materials processing fields, etc. The application of microwave energy to process various kinds of materials in an efficient, economic and effective manner is emerging as an innovative technology with great commercial potential and many advantages. Microwave processing is well recognised for many advantages over the conventional methods such as substantial enhancements in the reaction and diffusion kinetics, relatively much shorter cycle time, finer microstructures better quality products, and eco friendly etc.

In the areas of processing of ceramics and metals, it has been kind of sintering and synthesis revolution in terms of material diffusions and reaction kinetics. Until 2000, microwave processing of materials mostly was confined to ceramics, semimetals, inorganic and polymeric materials.

In 1999 Roy and co-workers [3] reported that a porous, powder metal compact could be heated and sintered in a microwave field. This was at that time considered surprising because the electrically conducting materials were supposed to reflect microwave radiation. Later on other researchers also demonstrates that all powder metals at room temperature absorb microwaves and only bulk metals reflect the microwaves allowing only surface penetration.

In the last few years many new developments in microwave processing of materials at high temperature have taken place in many countries worldwide. These developments include melting of metals and casting, steel making using microwave assisted technology, direct steel making using pure microwave technology and used tire reprocessing.

In this present investigation, attempts have been made to synthesize Cu-Cr alloy using as-received and milled Cr powder produced by planetary ball mill.

The structural and morphological changes of the milled samples are to be analyzed by various techniques, namely, XRD and SEM. Subsequently, powder mixture of Cu-Cr alloy separately using received Cr and as well as milled Cr powder were consolidated using uniaxial pressing to get three varying green density compacts.

Sintering was carried out using conventional method and microwave sintering technique at 1050 ºC for three different soaking periods. For microwave sintering, the design of unit was modified and developed to attain high vacuum pressure inside the chamber.

Microstructural analysis of the sintered specimens was also carried using SEM to compare the properties to that of the milled specimens. Measurement of physical properties like relative density, mechanical properties like Vickers hardness, and electrical properties like conductivity of all the sintered samples were investigated and compared with their conventional counter parts.

### 1.1 Aim and Objectives

With the above discussed background, the objectives of the present work are envisaged as:

- Design modification of microwave sintering unit to make it suitable for its usage at high vacuum.

- Reduction of size Cr particles by mechanical milling in WC grinding media by using planetary ball mill in order to get fine distribution of Cr in Cu matrix.
- Characterization of the ball-milled powder by XRD and SEM analysis.
- Consolidation and sintering of the green compacts using as-received and prepared milled powder by suitable techniques, namely, conventional sintering and microwave sintering.
- Characterization of microstructural features of the sintered compacts by SEM and Optical Microscope.
- Measurement of physical properties like density of the sintered specimens by Archimedes principle.
- Evaluation of mechanical properties and analysis of the sintered compacts.
- Evaluation of electrical conductivity of the sintered pellets.
- Analysis of the results and establishment of suitable composition for the best combination of mechanical and electrical properties for practical applications.

# Chapter 2 Literature Review

## 2.1 Vacuum Interrupters

In general, power distribution networks employ circuit breakers with different kind of protection devices in the main and sub feeders. These protection devices generally require vacuum interrupters (VIs) to control and protect the electrical distribution system. VIs are widely used for current interrupting in the low- and medium-voltage range (predominantly at 36 kV) based on their principle known since almost a century [4]. They have passed through many years of development and found worldwide acceptance due to their simple and compact structure as well as being maintenance-free for lifetime. Its basic function is to detect a fault condition and, by interrupting continuity, to immediately discontinue electrical flow. The internal components of a typical vacuum interrupter are shown in Figure 2.1

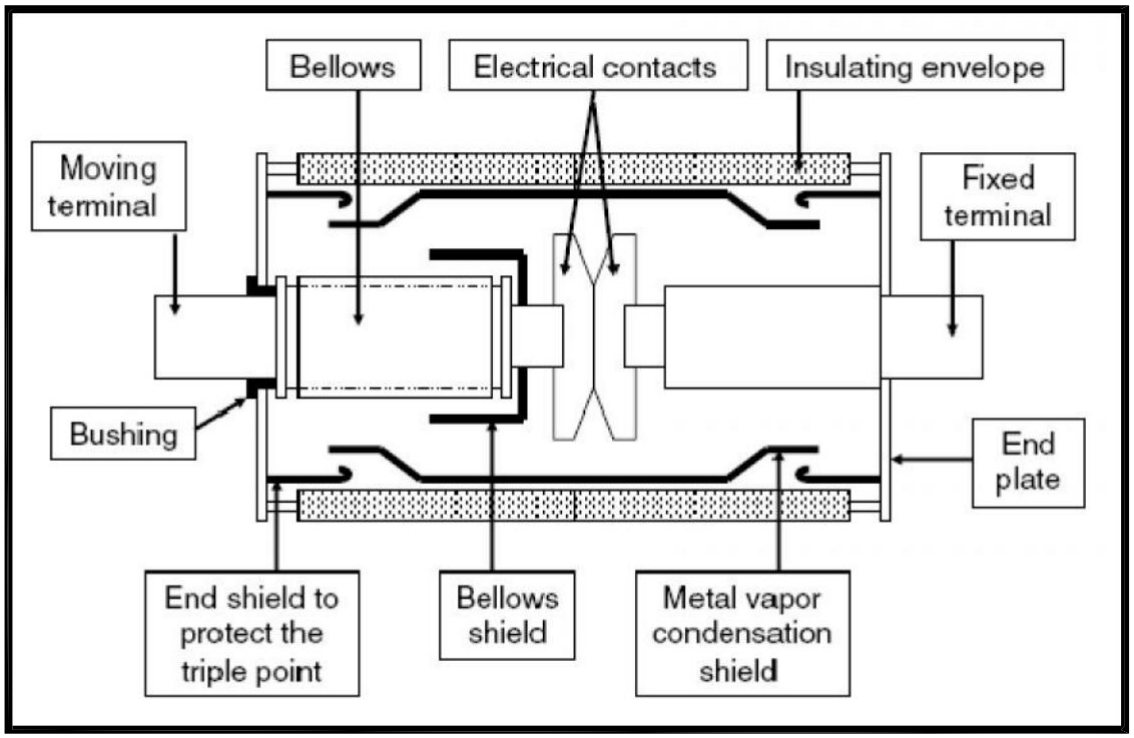


**Fig. 2.1**: The cross section of a vacuum interrupter [5].

Electrical contacts are one of the most important factors to determine the performance of VIs. Extremely pure and gas free contacts are housed in a vacuum chamber made up of a high alumina ceramic material. The contacts are closed by a mechanism connected to the moving terminal. The moving terminal is connected to the vacuum

(~ $10^{-6}$ mbar) chamber by a stainless steel bellows that permits the contacts to open and close while maintaining the vacuum. The vacuum offers some definite advantages to the designer of CMs as there is no gas to contaminate the contact surfaces.

### 2.1.1 Working principle for VIs

In its natural state, when the contacts touch each other the vacuum interrupter is said to be in the closed condition. Once a fault is detected, the contacts open by withdrawing the contact attached to the moving terminal from the contact attached to the fixed terminal and consequently a metal vapor arc is established within the interrupter. This arc, which consists exclusively of the vaporizing contact material, is sustained by the external supply of energy up until the next time the current passes through zero. At current zero, contact vapor production ceases, arc is finally extinguished and the vacuum interrupter regains its insulating capability which is to withstand the transient recovery voltage.

### 2.1.2 Problems associated with VIs

a) Arc Erosion: Within a few microseconds of arc initiation the temperature at the foot of the arc reaches extremely high values causing the metal at cathode to vaporize and transforming the metal to ion jets [6]. Therefore while interrupting high currents excess heat is generated and is to be dissipated by vapourization of material. To assure successful extinguishing at current zero any time, the contacts must be avoided to be strongly exposed to erosion by the vacuum arc during the high current phase.

b) Gas Evolution: The main problem with the vacuum interrupter is the evolution of gases from the contacts during arcing [7]. This gas evolution causes loss of vacuum with consequent degradation of breakdown and recovery characteristics of the interrupter.

c) Contact Welding: The arc so generated melt a small portion of contacts and thus under high mechanical forces, the contacts can get welded.

d) Current Chopping: During vacuum switching, under certain conditions, the current is cut off abruptly instead of coming to its natural zero along the normal sinusoidal path. This is known as current chopping and it arises because of the extremely good recovery characteristics of a vacuum gap. Depending on the circuit parameters the current chopping may constitute a direct overvoltage problem endangering the system

insulation. The chopping current of vacuum contact materials, which in turn depends on the composition, should not be too high.

## 2.2 Contact Materials for Vacuum Interrupters

The current interrupting capability of a vacuum interrupter depends on the contact material and its design. Microstructures of materials are the strategic link between materials processing and materials behaviour. Microstructure control is therefore essential for any process activity [8].

### 2.2.1 Property Requirements of Contact Materials

The following are some of the important requirements of contact materials used in vacuum interrupters:

- Low gas content and impurity degrees, to keep the vacuum during the whole service life.
- Good electrical conductivity to pass normal load currents without overheating and for reduction of permanent power losses.
- Good thermal conductivity for good heat removal during continuous load and for fast electrode cooling after current zero.
- Low and uniform erosion to give a long operating life.
- Sufficiently low vapour pressure to reduce the amount of metal vapour in the chamber
- High density
- Low chopping level
- Sufficient mechanical strength to resist any permanent deformations.
- Good interruption capability
- High electrical breakdown strength
- Good antiwelding properties

Most of the conventional materials could not meet all these requirements simultaneously [9]. For example tungsten has good vacuum dielectric and antiwelding properties. Its ability to interrupt high currents is however, rather disappointing. Copper, on the other hand, is quite good in interrupting high

currents and has also reasonably good vacuum dielectric strength. However it fails to meet the anti-welding requirements. The commonly used mixtures of silver-cadmium oxide are not acceptable for vacuum applications because of the presence of constituents with excessively high vapour pressure. Also, pure refractory metals show poor conductivity and cause heavy current chopping due to high heats of vapourization.

### 2.2.2 Vacuum Interrupter Materials

The commercial type materials that are made and used for vacuum interrupters can be divided into three groups [10]:

a) *Copper-Chromium Contacts* (a good conductor plus semi-refractory material). This type of material is currently the dominant material for circuit breaker. The composition ranges from 25 to 75% chromium. According to phase diagram of copper and chromium (Figure 2.2), both components are completely soluble into each other in liquid phase. However chromium separates from oversaturated copper under cooling to ambient temperatures. The mixing ratio of copper and chromium can be adjusted within wide range due to good wettability of chromium caused by the low solubility of chromium in the copper phase. Both form an eutectic at 1076 $^{o}$C with 1.56 atom % chromium.

*b)* *Tungsten-copper or tungsten carbide-silver* (refractory material plus a good conductor). The mixture of W and Cu has long been used for switching low currents in high-voltage circuits. More recently, the WC-Ag contact, with its low surge capability, has found wide use in low-voltage contactors. As a result of interruption limitation this class of material is usually limited to lower-current vacuum interrupter designs

*c)* *Copper-bismuth alloy.* Copper with a small amount of bismuth was popular material for vacuum interrupters in the late 1960s. The small amount of bismuth gave the material gave good dynamic weld resistance properties. In general this material has been replaced by chromium copper.

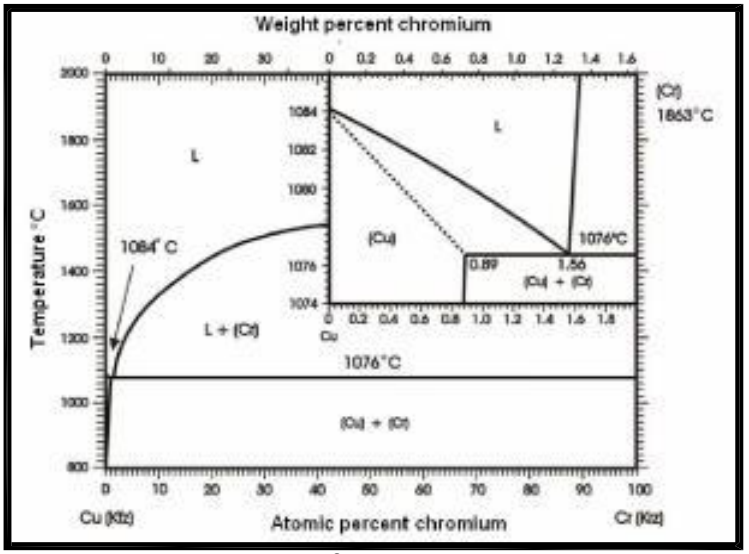


**Fig. 2.2**: Phase diagram of copper and chromium [11].

### 2.2.3 Development of Copper-Chromium Contact Material

In power delivery engineering, Cu-Cr have been accepted and adopted for VCB by the early 1990s, and up to now they are still dominant materials for VCB worldwide because of unique combination of properties of two constituents. It combines good electrical properties with outstanding circuit interruption ability and excellent arc erosion and welding resistance.

Four manufacturing techniques are used to produce Cu-Cr contact materials: arc-melting, vacuum casting, infiltration and sintering techniques [2]. Cu-Cr sintering contact material was first proposed and adopted for VI by A. A. Robinson and his colleagues in English Electric Corporation, UK in1970 [12]. About fifteen years later Horst Kippeenberg et al. [13] developed vacuum infiltration Cu-Cr contact materials and successfully used it for VCB. Soon afterwards, the arc-melting Cu-Cr alloy contact materials were developed by R. Muller in 1988 [14]. Schellekens et al [15] reported the experimental results of the plasma sprayed Cu-Cr alloys and gave some comparisons with the conventional Cu-Cr alloys. Vacuum Induction Melting and Rapid Solidification Cu-Cr alloy contact materials were developed by Baihe Miao in 1998 [2]. Adopting what sort manufacturing technique to produce contact materials will determine strongly their quality and microstructure, properties and performance level.

In 1989 Rieder et al. [16] experimentally proved that fine Cr particles tend to decrease the maximum chopping currents and the breakdown voltage is significantly higher for

contacts incorporating the finer Cr particle sizes. In 1999 Wang et al. [17] experimentally showed that the high voltage withstandability of the nanocrystalline Cu-Cr materials in vacuum is much higher than those of microcrystalline materials prepared by the same procedures. Yongxing [18] suggested the cryogenic process is effective in improving the properties of the Cu-Cr contact materials. Fink et al. [19] established a new contact material based on multilayer system to improve various properties. It turned out that the higher thermal and electrical conductivity as well as mechanical properties of the multilayer contact material improved interruption ability of the VI. Lahiri [20] performed explosive compaction of mechanically alloyed Cu-Cr powder followed by solid-state sintering which showed best combination of properties such as excellent density and exceptionally high electrical conductivity.

## 2.3 Mechanical Milling

Mechanical Milling (MM) is the most widely used method of powder production for hard metals and oxide powders. It is a process of comminution of uniform (often stoichiometric) composition powders, such as pure metals, intermetallics, or prealloyed powders to a small size by using high-energy ball-milling, where material transfer is not required for homogenization [21-23]. It involves repeated deformation, cold-welding, fracturing, and dynamic recrystallization to achieve an extremely fine grain size. Besides particle size reduction, it associates with particle size growth, particle shape change, agglomeration, solid-state alloying (mechanical alloying) and solid-state blending. MM is most extensively used for non-equilibrium processing of metastable phases such as amorphous alloys, extended solid solution, and to synthesize nanostructured materials. [24-27].

### 2.3.1 Principle of Milling

During milling, four types of forces act on particulate material: impact, attrition, shear, and compression. Impact is the instantaneous striking of one object by another. Attrition is the production of wear debris or particles created by the rubbing action between two bodies. This type of milling force is preferred for those materials which can be easily broken up and exhibits minimal abrasiveness. Shear consists of cutting or cleaving of particles and usually is combined with other types of force. Shear

contributes to fracturing by breaking particles into individual pieces with a minimum of fines. Compression is the crushing or squeezing of particulate material and also the breaking of large agglomerates of hard, non-ductile material. [28]

Whenever two steel balls collide, some amount of powder is trapped in between them (Figure 2.3). During high-energy milling the powder particles are repeatedly flattened, cold welded, fractured and rewelded. The force of the impact plastically deforms the powder particles leading to work hardening and fracture. The new surfaces created enable the particles to weld together and this leads to an increase in particle size. Since in the early stages of milling, the particles are soft (ductile), their tendency to weld together and form large particles is high. With continued deformation, the particles get work hardened and fracture by a fatigue failure mechanism and/or by the fragmentation of fragile flakes. Fragments generated by this mechanism may continue to reduce in size in the absence of strong agglomerating forces. At this stage, the tendency to fracture predominates over cold welding. Due to the continued impact of grinding balls, the structure of the particles is steadily refined, but the particle size continues to be the same. After milling for a certain length of time, steady-state equilibrium is attained when a balance is achieved between the rate of welding, which tends to increase the average particle size, and the rate of fracturing, which tends to decrease the average particle size. Thus it is important to determine the time required for a process to reach equilibrium particle size and the milling process should be terminated at that point.

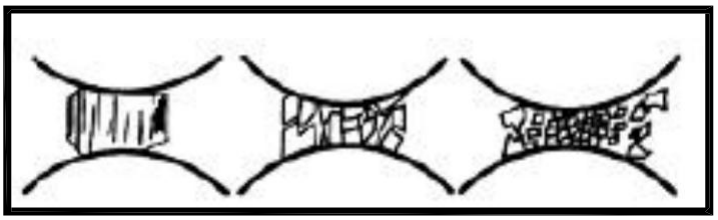

**Fig. 2.3**: Ball-powder-ball collision of powder during mechanical milling.

### 2.3.2 Process Variables

Mechanical Milling involves optimization of a number of variables to achieve the desired results. Some of the important parameters that have an effect on the final constitution of the powder are:

- Type of mill
- Milling container

- Milling speed
- Milling time
- Type, size, and size distribution of the grinding medium
- Ball-to-powder weight ratio
- Extent of filling the vial
- Milling atmosphere
- Process control agent

All these process variables are not completely independent. For example, the optimum milling time depends on the type of mill, size of the grinding medium, temperature of milling, ball-to-powder ratio, etc.

**Type of mill**

During milling, the motion of milling medium and charge varies between types of mills, with respect to movement and trajectories of individual balls, movement of the mass of balls, and the degree of energy applied to impact, shear, attrition, and compression forces acting on powder particles. They also differ in their capacity, efficiency of milling and additional arrangements for cooling, heating, etc. There are a number of different types of mills for conducting MM, for example shaker mills, Planetary ball mills, Attritor mills etc.

But the most popular mill for conducting MM is the planetary ball mill in which a few hundred grams of the powder can be milled at a time. The planetary ball mill owes its name to the planet-like movement of its vials. These are arranged on a rotating support disk and a special drive mechanism causes them to rotate around their own axes. The centrifugal force produced by the vials rotating around their own axes and that produced by the rotating support disk both act on the vial contents, consisting of material to be ground and the grinding balls. Since the vials and the supporting disk rotate in opposite directions, the centrifugal forces alternately act in like and opposite directions. This causes the grinding balls to run down the inside wall of the vial - the friction effect, followed by the material being ground and grinding balls lifting off and travelling freely through the inner chamber of the vial and colliding against the opposing inside wall - the impact effect.

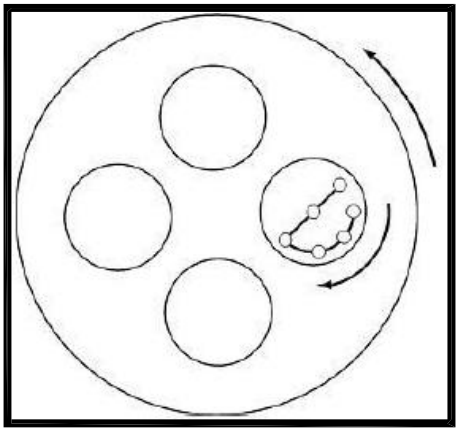

**Fig. 2.4**: Schematic drawing of a planetary ball mill.

**Milling Container**

Due to impact of the grinding medium on the inner walls of the container, some material will be dislodged and get incorporated into the powder. If the material of the grinding vessel is different from that of the powder, then the powder may be contaminated with the grinding vessel material. On the other hand, if the two materials are the same, then the chemistry may be altered unless proper precautions are taken to compensate for the additional amount of the element incorporated into the powder. Hardened steel, tool steel, hardened chromium steel, tempered steel, stainless steel, WC-Co, WC- lined steel and bearing steel are used for the grinding vessels.

**Milling Speed**

The efficiency of milling increases with increase in speed. But it shouldn't exceed critical speed of the mill. Above a critical speed, the balls will be pinned to the inner walls of the vial and do not fall down to exert any impact force. Therefore, the maximum speed should be just below this critical value. Another limitation to the maximum speed is the temperature rise during milling.

**Milling Time**

The time of milling is the most important parameter. Normally the time is so chosen as to achieve a steady state between the fracturing and cold welding of the powder particles. The times required vary depending on the type of mill used, the intensity of milling, the ball-to-powder ratio, and the temperature of milling. The level of contamination increases with milling time and some undesirable phases form.

Therefore, it is desirable that the powder is milled just for the required duration and not any longer.

**Grinding Medium**

Hardened steel, tool steel, hardened chromium steel, tempered steel, stainless steel, WC-Co, and bearing steel are the most common types of materials used for the grinding medium. The density of the grinding medium should be high enough so that the balls create enough impact force on the powder. It is always desirable to have the grinding vessel and the grinding medium made of the same material as the powder being milled to avoid cross contamination.

The size of the grinding medium also has an influence on the milling efficiency. It has been reported that a combination of large and small size balls during milling minimizes the amount of cold welding and the amount of powder coated onto the surface of the balls.

**Ball-to-powder weight ratio (BPR)**

The ratio of the weight of the balls to the powder (BPR), sometimes referred to as charge ratio, is an important variable in the milling process. The minimum BPR ranges from as low as 1:1 to as high as 220:1. The BPR has a significant effect on the time required to achieve a size of powder being milled. The higher the BPR, the shorter is the time required. In general ratio of 10:1 is most commonly used while milling the powder.

**Extent of filling the vial**

Since comminution of the powder particles occurs due to the impact forces exerted on them, it is necessary that there is enough space for the balls and the powder particles to move around freely in the milling container. Thus, care has to be taken not to overfill the vial; generally about 50% of the vial space is left empty.

**Milling Atmosphere**

Different atmospheres have been used during milling for specific purposes. A nitrogen atmosphere is used to produce nitrides. Similarly, hydrogen atmosphere is used to produce hydrides. The presence of air in the vial has been shown to produce

oxides and nitrides in the powder, especially if the powders are reactive in nature. High- purity argon is the most common ambient to prevent oxidation and/or contamination of the powder.

**Process Control Agent**

A process control agent (PCA) is added to the powder mixture during milling to reduce the effect of cold welding. The nature and quantity of the PCA used and the type of powder milled would determine the final size, shape, and purity of the powder particles. Use of a larger quantity of the PCA normally reduces the particle size by 2-3 orders of magnitude [29]. The amount of the PCA is dependent upon the (a) cold welding characteristics of the powder particles, (b) chemical and thermal stability of the PCA, and (c) amount of the powder and grinding medium used. The most important of the PCAs include stearic acid, hexane, toluene, methanol, and ethanol.

## 2.4 Microwave Sintering

Microwave Sintering has emerged in recent years as a new method for sintering a variety of materials. It has shown significant advantages against conventional sintering procedures. The use of microwaves to materials processing was studied intensively in the 1970s and 1980s, and initial success in microwave heating and sintering was confined mainly to oxide and some non-oxide ceramics. The most recent development in microwave applications is in sintering of metal powders, a surprising application because metallic materials reflect microwaves. However, in 1999, Agrawal et al. [3] first reported that microwave enhance the sintering of metallic materials to full density. Furthermore, Cheng et al. [30] demonstrated that metals are heated well in the magnetic field of microwave. Now, it has been found that the microwave sintering can also be applied as efficiently and effectively to powdered metals as to many ceramics. Metal in the form of powder will absorb microwaves at room temperature and will be heated very effectively and rapidly. This technology can be used to sinter various powder metal components.

Microwave energy is a form of electromagnetic energy with the frequency range of 300MHz to 300 GHz. The basic perspective of using microwave energy is to generate

heat directly in the object itself and possibly create a uniform temperature distribution. In Microwave Heating, material interacts with microwaves, absorb the electromagnetic energy volumetrically, and transform into heat. This is different from conventional methods where heat is transferred between objects by the mechanisms of conduction, radiation and convection. In conventional heating, the material's surface is first heated followed by the heat moving inward. This means that there is a temperature gradient from the surface to the inside. However, microwave heating generates heat within the material first and then heats the entire volume [31]. This heating mechanism offers many advantages, that have not been observed in conventional heating, in terms of enhanced diffusion processes, reduced energy consumption, very rapid heating rates and considerably reduced processing times, decreased sintering temperatures, improved physical and mechanical properties, simplicity, unique properties, and lower environmental hazards [32]. However, due to the complexity of microwave interactions with materials, microwave processing has not always been as successful as enthusiasts of the technology had hoped. The successful application of microwave processing places a heavier demand on the user to understand the technique than does conventional heating. Materials processors are becoming more sophisticated at tailoring the material to the manufacturing process in order to make full use of the capabilities of microwaves

### 2.4.1 Theoretical Aspect of Microwave Sintering

Microwave energy is a form of electromagnetic energy with the frequency range of 300MHz ($3\times10^8$ cycles/s) to 300GHz ($3\times10^{11}$ cycles/s) and the corresponding wavelengths are between 1mm and 1m. The frequency and wavelength range of microwaves are shown in Figure 2.5. Microwaves have longer wavelengths and lower available energy quanta than other forms of electromagnetic energy such as visible, ultraviolet or infrared light.

Typical frequencies for material processing are 915 MHz, 2.45 GHz, 5.8 GHz, and 24.124 GHz. These frequencies are chosen for the microwave heating based on two reasons. The first is that they are in one of the industrial, scientific and medical (ISM) radio bands set aside for non-communication purposes. The second is that the penetration depth of the microwaves is greater for these low frequencies [33]. Also,

Microwaves are coherent and polarized and can be transmitted, absorbed, or reflected depending on the material type [34].

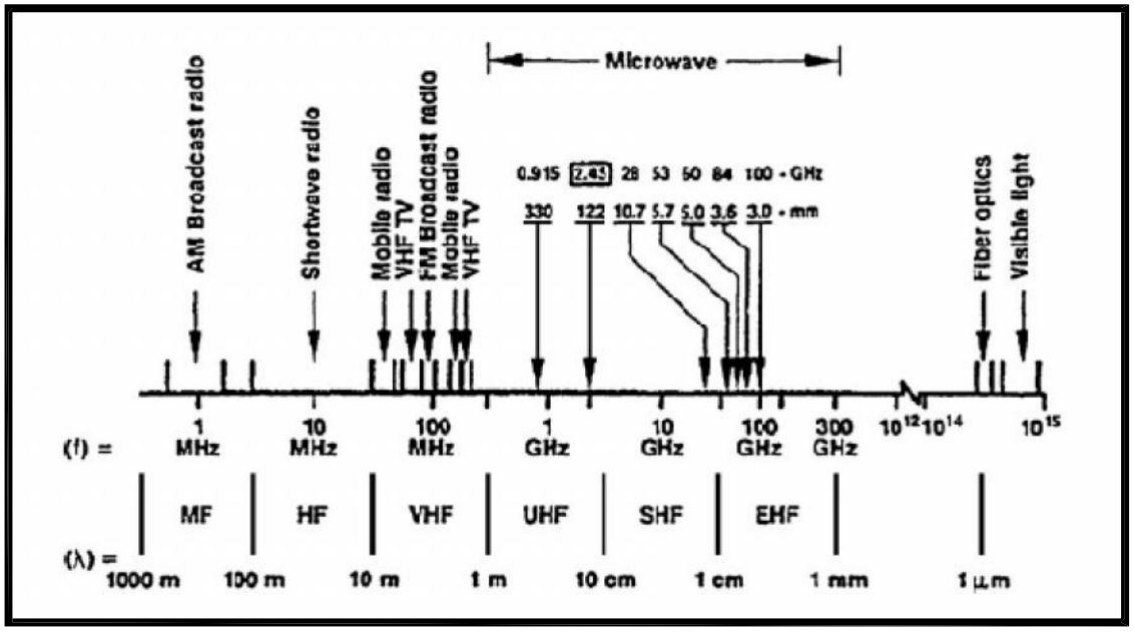


**Fig. 2.5**: Electromagnetic spectrum and frequencies used in microwave processing.

Microwave propagation in air or in materials depends on the dielectric and the magnetic properties of the medium. The electromagnetic properties of a medium are characterized by complex permittivity (ε) and complex permeability (μ), where:

$$\varepsilon = \varepsilon' - i\,\varepsilon'' \tag{2.1}$$

$$\mu = \mu' - i\,\mu'' \tag{2.2}$$

The complex permittivity is a measure of the ability of a dielectric to absorb and to store electrical potential energy. The real component of complex permittivity, $\varepsilon'$, is commonly referred to as the dielectric constant; not constant but can vary significantly with frequency and temperature, it is simply known referred as permittivity. The imaginary components of complex permittivity, $\varepsilon''$, is the dielectric loss factor. Similarly, the real and imaginary components of the complex permeability, $\mu'$ and $\mu''$, are permeability and magnetic loss factor, respectively. The quantity tan δ is the loss tangent, the most important parameter in microwave processing, which indicate the ability of the material to be polarized and heated. It can be expressed as Equation 2.3.

$$\tan\delta = \frac{\varepsilon''}{\varepsilon'} \tag{2.3}$$

The loss factor measures the ability of the material to transfer microwave energy into heat and the dielectric constant measures the ability of the material to be polarized [34]. A material with high tan δ and $\varepsilon''$ heats more effectively than a material with low tan δ and $\varepsilon''$. For optimum coupling, a balanced combination of moderate $\varepsilon'$ to permit adequate penetration and high loss (maximum $\varepsilon''$ and tan δ) are required.

Absorbed power (P) and penetration depth (D) are two important parameters which will determine the uniformity of heating throughout the material. The average absorbed power, P, which is volumetric absorption of microwave energy ($W/m^3$) in material, is expressed as Equation 2.4 [33].

$$P = 2 \pi f \varepsilon_0 \varepsilon'_r \tan \delta E^2 \qquad (2.4)$$

The penetration depth D determines the depth of penetration at which the incident power is reduced by one half exhibiting the uniformity of heating throughout the material. Higher the values of tan δ and $\varepsilon'_r$, smaller is the depth of penetration for a specific wavelength. High frequencies and large values of the dielectric properties will result in surface heating, while low frequencies and small values of dielectric properties will result in more volumetric heating [34].

For a conductive metallic material, an incident wave is mainly reflected, and the rest cannot pass through the superficial layer of the metal itself. The penetration depth of the microwaves at a given frequency depends on the electrical and magnetic properties of the material and is a very important parameter, because it constitutes an upper limit to the thickness of the material which can be heated directly by microwaves. The skin depth "d" (m) is defined as the depth into the conductor from the surface at which the current density is 1/e (36.8%) of its value at the surface [35], given by equation 2.5.

$$d = \left( \frac{1}{\pi f \sigma \mu a} \right)^{½} \qquad (2.5)$$

Materials with high conductivity and permeability present a lower penetration depth, for a given frequency, but there is also implicit temperature dependence due to the changes of σ and $\mu_a$. Most metals generally have a skin depth of the micrometer order, so the direct heating tends to remain superficial, but using powders with particle size

of the skin depth order, it is possible to heat them directly and use microwave in the sintering process [36].

As seen from the above equations, the dielectric properties ($\varepsilon_0$, $\varepsilon'$ and tan $\delta$) act as an important role in the extent of power absorbed by a material.

### 2.4.2 Microwave Sintering Versus Conventional Sintering

Microwave sintering is fundamentally different from conventional sintering. In conventional methods, sintering of materials is done by mixing of material powder with or without additives and pressing into green (metals or ceramics) parts followed by sintering with indirect heating of green pellets at about 0.6-0.8 $T_m$ in a refractory type electrical resistance or induction furnace whereas Microwave Sintering provide direct heating of the green part.

In terms of heating mechanism, in conventional sintering heat transfer takes place to the surface of the material by radiation or convection heating that is transferred to the bulk of material via conduction. It is rather a slow process and takes considerable time to achieve thermal equilibrium and material consolidation. It is independent of the nature of the material. On the other hand, Microwave Sintering is the transfer of electromagnetic energy to thermal energy and is energy conversion rather than heat transfer. During the microwave sintering procedure, materials themselves absorbs microwaves such that electromagnetic energy of the microwaves is converted to thermal energy and heat can be generated throughout the volume of the material resulting in volumetric heating. Microwave heating is instantaneous and rapid, and depends on a variety of factors such as size, geometry, mass and dielectric property of the sample.

The thermal gradient in the microwave-processed material is the reverse of that in the material processed by conventional heating. In a conventional heating, the direction of heating is from outside to inside of the powder compact resulting in higher temperature of the sample surface than core while for microwaves, the direction of microwave heating is from inside to outside of the powder compact resulting in higher temperature of the sample core than the surface. The temperature profile for both methods is shown in Figure 2.6. The former mode of heating results in poor

microstructural characteristics of the core of the powder compact while the latter results in poor microstructural characteristics of the surface [31].

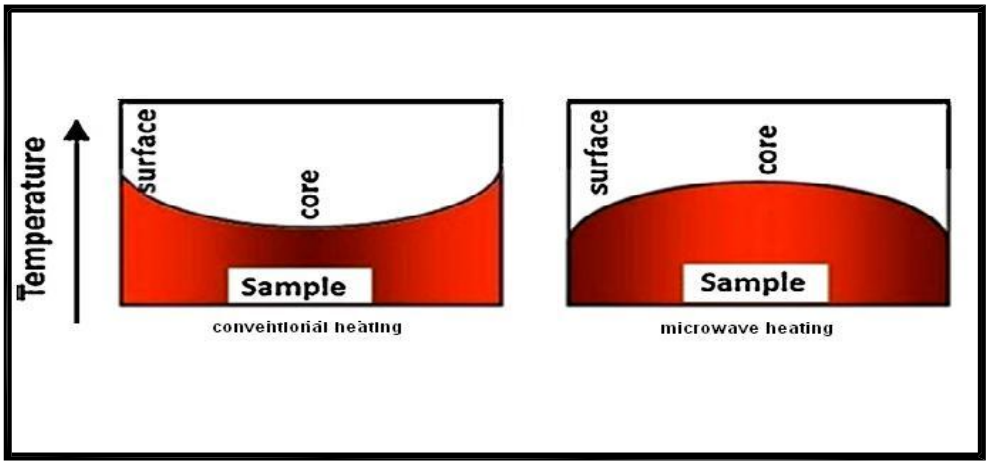


**Fig. 2.6**: Temperature profile within the sample in conventional heating and microwave heating [32].

A remarkable energy and time saving can be obtained with microwave sintering. Furnaces for conventional sintering use a large number of expensive heating elements, fuel and refractory materials to achieve and maintain the high temperature for a long time; therefore it consumes much electrical energy and much fuel. As microwaves facilitates the direct transfer of energy into the materials, it eliminates wasting of energy by simultaneous heating of furnace and heat carriers and also offers the potential of applying high heat-up rates.

In conventional heating, slow heating rates are selected to prevent thermal gradient at high sintering temperatures which otherwise lead to compact distortion and inhomogeneous microstructure. Consequently, to reduce steep thermal gradient by a slower heating rates, which increases the process time, it contributes to microstructural coarsening [37]. Despite restricting microstructural coarsening, microwave processing reduces typical sintering times by a factor of 10 or more in many cases [38].

Microwave sintering technique can effectively promote the forward diffusion of ions and thus accelerate the sintering process, resulting in the grain growth and the densification of matrix [32]. Because it is a non-contact technique and the heat is transferred to the product via electromagnetic waves, large amount of heat can be transferred to material's interior minimizing the effects of differential sintering [39]. In many cases, the microwave sintering has shown to produce samples with more

uniform grain size distribution, much finer average grain size and higher density; result in enhanced mechanical properties with respect to conventional treated ones [40].

### 2.4.3 Interactions between Microwaves and Materials

When an electric field interacts with a material, various responses may take place. Based on the microwave matter interaction, most materials can be divided into three categories as shown in Figure 2.7: (a) transparent, which are low dielectric loss materials where microwaves pass through without any losses: (b) opaque (bulk metals), where microwaves are reflected and cannot penetrate; and (c) absorbing, which are high-loss materials where microwaves are absorbed depending on the value of the dielectric loss factor. However, metals in powder form are very good absorbers of microwaves and get heated very effectively. Further, bulk metals, if pre-heated to moderate temperatures (~500$^{\circ}$c), also become good microwave absorbers. Most other materials are either transparent or absorb microwaves to varying degrees at ambient temperature depending upon their inherent electrical and magnetic properties. The degree of microwave absorption and consequent heating profile changes dramatically with the rise in temperature. Microwave heating is material dependent; therefore only those materials that couple in the microwave field will get heated and the rate of heating will depend upon their degree of absorption, which is a function of various factors including the dielectric loss (insulators), magnetic properties (metals), grain size, porosity, frequency, electrical conductivity, etc [41]. There can be also a fourth type of interaction which is observed in composite or multi-phase materials where one of the phases is a high-loss material while the other is a low-loss material [32].

### 2.4.4 Application of Microwave Sintering in Engineering Materials

Microwave energy has been in use for variety of applications for over 50 years. These applications include communication, food processing, wood drying, rubber vulcanization, medical therapy, polymers, etc. Microwave processing of materials was mostly limited until 2000 to ceramics, semiconductors, inorganic and polymeric materials. However, now it has been shown that the microwave energy can be used to sinter virtually all powdered metals as efficiently and effectively as in the ceramic systems. This has opened up an entirely new research area to investigate the advantages of microwaves for metallic materials to meet the challenging and growing

needs in many metallurgical applications. The following demonstrates microwave sintering advantages against conventional sintering for some important engineering materials.

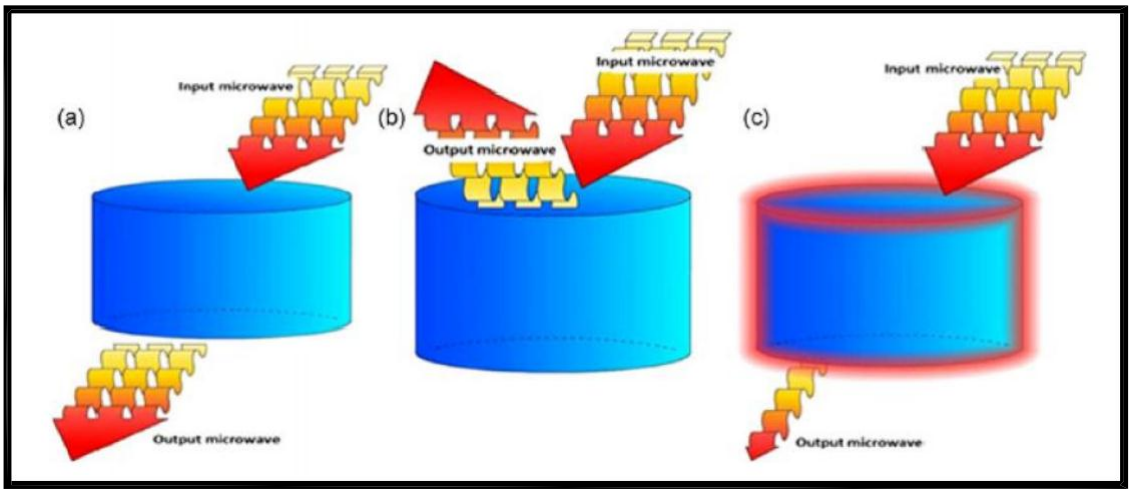


**Fig. 2.7**: Three kinds of materials according to the interaction with microwaves: (a) transparent, (b) opaque (conductor) and (c) absorber [32].

The following demonstrates microwave sintering advantages against conventional sintering for some important engineering materials.

**a) Ceramics**

Many traditional and advanced ceramics have been processed by microwave with reported enhancements in reaction, and diffusion kinetics exhibiting better properties than the conventionally processed material.

1) Alumina ($Al_2O_3$)

Alumina is the most common ceramic and because of its highly refractory nature it is difficult to sinter it to full densification unless suitable sintering aids or some special processing techniques are adopted. Cheng at al. successfully sintered transparent alumina samples by microwaves [42]. In the conventional sintering processes, extremely high sintering temperatures (up to 1900 ºC) and long soaking times (several hours) under high vacuum or pure hydrogen atmosphere are applied in the fabrication of transparent alumina products to achieve the highest density and minimum porosity. Figure 2.8 shows the microstructure of the sample microwave sintered at 1750 ◦C with dwelling time of 45min. As can be seen from figure, the sample exhibits very neat grain boundary structure and uniform grain growth with no porosity. Microwave-

sintered samples with dwelling time of 15–45 min had the same density of 3.97 g/cm$^3$ (~100% of theoretical density).

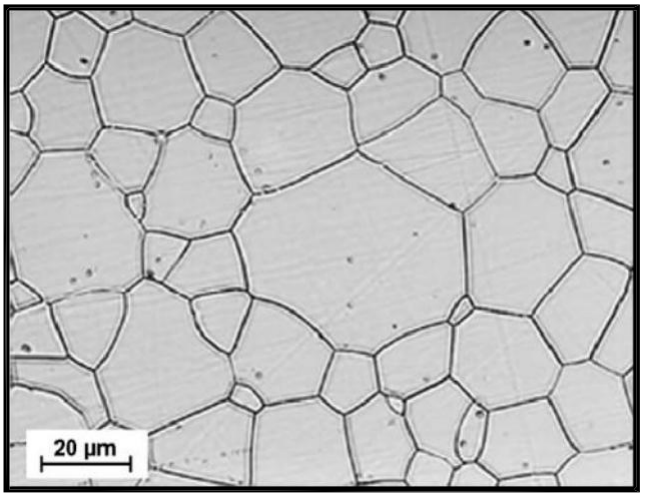


**Fig. 2.8**: Microstructures of the $Al_2O_3$ sample microwave sintered at 1750º C for 45 minutes [42].

2) Zirconia

Zirconia being a refractory oxide ceramic often requires high sintering temperatures and soaking time to obtain high degree of densification. In microwave fine grained zirconia ceramics were sintered at 1360 ºC/2 min in a multimode, 2.45 GHz system. The sintered density was ~97.8% and average grain size was 0.25 mm. Binner et al. [43] reported the fabrication of transparent zirconia ceramics using nanopowder and microwave hybrid heating at 1600C. Figure 2.9 displays the SEM photograph of a typical transparent zirconia sample prepared by microwave hybrid heating. The use of microwave hybrid heating had resulted in a much finer average grain size at all densities.

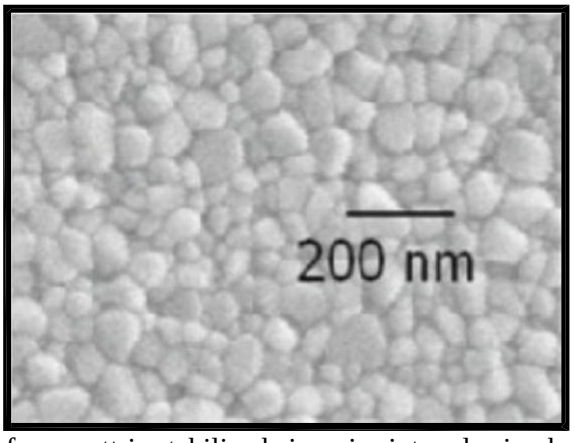


**Fig. 2.9**: Microstructure of nano yttria stabilized zirconia sintered using hybrid microwave sintering [43].

3) ZnO based ceramic varistor

Zinc oxide varistors are electronic ceramic devices possessing highly non-linear current voltage characteristics, which enable them to be used as voltage surge suppressors. Various types of zinc oxide varistors under different processing conditions were sintered using microwave heating [44]. Microwave sintering of ZnO varistor samples indicates significant reduction in the cycle time and substantial improvements in the electrical properties. They exhibited better densities, finer grain size, and more uniform microstructure relative to conventional process (Figure 2.10). Electrical characterizations of the microwave sintered samples showed higher volts and better clamping properties as compared to the conventional sintering.

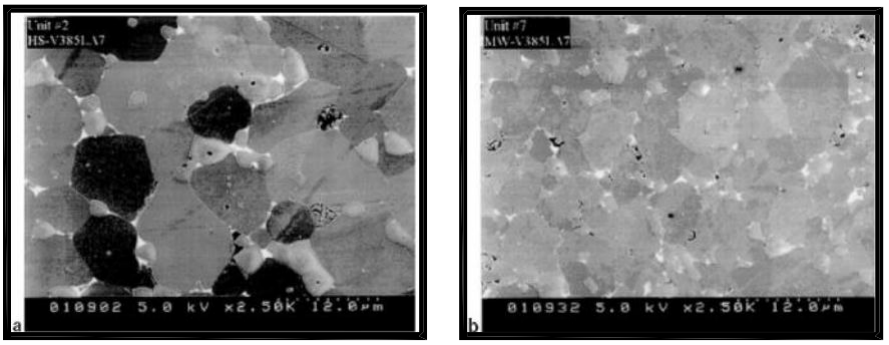


**Fig. 2.10**: Microstructures of a) conventional and b) microwave sintered ZnO based varistor samples [44].

**b) Metals**

Now it has been found that the microwave sintering can also be applied as efficiently and effectively to powdered metals as to many ceramics, many commercial powder-metal components of various alloy compositions including iron and steel, copper, aluminum, nickel, Mo, Co, Ti, W, Sn, etc., and their alloys have been sintered in microwaves producing better properties than their conventional counterparts.

1) Austenitic (316L) and ferritic (434L) stainless steel

Panda et al. compared the effect of heating mode on the sintering time, densification, microstructure, strength and hardness of 316L (austenitic) and 434L (ferritic) stainless steel [37]. About a 90% reduction in the process time was shown for the sintering of stainless compacts in a microwave furnace. For both types of stainless steel, microwave sintering restricts microstructural coarsening. For both stainless steels, microwave sintering results in a smaller and narrower pore size distribution.

2) Tungsten Powder

Conventional sintering of the highest melting point metal, tungsten powder, requires high sintering temperatures (T > 2773 K) and relatively long soaking times to achieve densities above 90% of theoretical density. Microwave sintering of as-received tungsten powder of 99.95% purity and average particle size of 5–7 μm and activated tungsten powder by reducing its particle size in a high-energy planetary mill with milling time of 5 hour and plate and bowl speed of 240 and 670rpm is carried out in a 3 kW, 2.45GHz microwave furnace. Both the powder compacts are sintered under identical conditions. Maximum sintering temperature was 2073 K. While the as-received powder got densified to 85% of theoretical density (TD), the density of the compact made from activated powder is calculated to be 93% of TD. Vickers Hardness measurements showed higher hardness of 303 VHN for activated tungsten against 265 VHN for as-received tungsten. The maximum power consumption for the whole process was 20kW and the processing time was well within 6–7 hour [45].

3) Copper Powder

Mondal et al. [46] describes how the thermal profile of electrically conductive powder metal like copper changes with particle size and also with porosity content when the material is exposed to 2.45 GHz microwave radiation in a multimode microwave furnace. Pure copper powders with varying mean sizes (6 to 383 μm) and having a range of initial porosity (24 to 44%) effectively coupled with microwaves and heated to high temperatures. The smaller the powder size, the higher the heating rate. At the same power level, compacts having higher porosity heat at faster rates.

# Chapter 3 Experimental Procedure

This chapter deals with the details of the experimental procedures carried out in this investigation. To ensure the validity of the reported measurements, all equipments were calibrated for precision and accuracy. The measurements were performed according to standardized protocols to ensure repeatability.

## 3.1 Powders

For the present study, Copper-Chromium alloy of composition Cu-75% and Cr-25% (by weight) was selected. Powders used in the experiments were electrolyzed Cu and electrolyzed Cr. The as-received powders were characterized for their size, size distribution and morphology. Table 3.1 summarizes the characteristics of the elemental Cu & Cr powders used for this study.

**Table 3.1**: Powder characteristics of as-received condition.

| | **Powder** | |
|---|---|---|
| | **Cu** | **Cr** |
| **Supplier** | Pometon, Italy | JMC, Japan |
| **Fabrication Method** | Electrolytic | Electrolytic |
| **Purity** | 99.65 % | 99.0% |
| **Size** | -325 mesh | -325 mesh |
| **Theoretical Density, g/cc** | 8.9 | 7.1 |
| **Melting Point ºC** | 1083 | 1907 |

## 3.2 Mechanical Milling of Chromium Powder

In the present investigation, mechanical milling of chromium was carried out to reduce the powder particle size. Elemental chromium powder was milled for 9 and 18 hours in an in-house built planetary ball mill (Figure 3.1), using hardened steel vial. Balls used were made of tungsten carbide (WC) with 10 mm diameter. The ball to powder weight ratio and milling speed were 10:1 and 120 rpm, respectively. Toluene was used as the process control agent. The milling was carried out under protective atmosphere of purified argon (99.995 %) to prevent oxidation. The characterization techniques used for the present investigation have been described in the following section.

**Fig. 3.1**: Planetary Ball Mill used for Mechanical Milling

## 3.3 Characterization of Milled Powder

### 3.3.1 Particle Size and Shape

The measurement of particle size was carried out using a laser-scattering size analyzer (model: Mastersizer 2000, supplier: Malvern, UK). The technique is based around the principle that particles passing through a laser beam will scatter light at an angle that is directly related to their size. As the particle size decreases, the observed scattering angle increases logarithmically. The observed scattering intensity is also dependent on particle sizes and diminishes, to a good approximation, in relation to the particle's cross-sectional area. Large particles therefore scatter light at narrow angles with high intensity, whereas small particles scatter at wider angles but with low intensity. A low-angle Fraunhofer light scattering using monochromatic (laser) light was used in the present case. The technique requires dispersed particles, thus, a suspension was made adding about 3 g of powder in a 10 wt. % solution of sodium pyrophosphate. The particles are passed through the laser beam in a circulating water stream.

A scanning electron microscope (model: Quanta 200, supplier: FEI, USA) was used for the morphology, particle size and microstructural characterization of different hours milled powder. Micrographs are taken at suitable accelerating voltages for the best possible resolution using the Large Field Detector (LFD) imaging mode.

### 3.3.2 BET Surface Area

Surface area of as-received and milled Cr powder were calculated using a Smart Sorb 92/93 surface area analyzer (Figure 3.2). The instrument Smart Sorb 92/93, a surface area analyser, is based on the theory first proposed by Brunaur, Emmet and Teller known as BET theory. The instrument measures the surface area of solid particle samples over a wide range by non destructive method. The basic principle of instrument is that a gas mixture of 70% He & 30% $N_2$ is passed over the sample where $N_2$ in this mixture gets adsorbed over the surface of sample when it is dipped in liquid nitrogen. This adsorbed $N_2$ is allowed to desorb by bringing the sample to room temperature which is proportional to the surface area.


**Fig. 3.2**: Smart Sorb 92/93 surface area analyzer

### 3.3.3 Apparent Density

The apparent density of the powder gives a measure of the degree of packing of the powder in loose form. It is generally expressed as a fraction of the theoretical density. Apparent density measurements of the powders were carried out using an Hall flow meter according to the MPIF specification 4. The technique involves filling the powder in a brass bushing (inner diameter: 2.5 mm). The bushing is slid across a steelblock having a cylindrical cavity with 25 $cm^3$ volume. The weight of the powder in the cavity divided by the cavity volume gives the apparent density. Apparent density provides an estimate of the total volume occupied by a loose (non-vibrated) powder mass.

### 3.3.4 XRD analysis

The phase evolution at different stages of mechanical milling were studied by XRD analysis using the Cr Kα (λ= 2.2896) in a Philips X-pert MPD X-ray diffractometer. XRay diffraction patterns were recorded from 20° to 120° with an accelerating voltage of 40 kV. Data were collected with a counting rate of 2°/min. The average crystallite size of as-received and milled Cr powder was determined from the broadening of Cr reflection. For the overlapping peaks, the full-width at half intensity maximum and the true Bragg angle (2θ) were determined by an appropriate deconvolution exercise.

## 3.4 Powder Mixing

Elemental powders were weighed to 0.001 g accuracy using an electronic balance (model: AE 200, supplier: Mettler, Switzerland). The balance was calibrated using a series of standard weights. The alloy composition as mentioned before of copper comprising 75% by weight and Chromium of 25% by weight were prepared by mixing the required proportions of each powder in a V-cone blender for 15 min. Mixing ensures complete homogeneity in the powder mixture. To prevent segregation, due care was taken to make sure that the mixed powders were not shaken after mixing. Three blended mixtures were prepared comprising Copper and Cr powder as received, Copper and 9 hours milled Cr Powder and Copper and 18 hours milled.

## 3.5 Compaction

Three blended mixtures were compacted using a uniaxial semi-automatic hydraulic press (model UTM 60, supplier FIE, India) in to a cylindriczal pellet (29.5 mm diameter and 8 mm average height). Samples were compacted under variable loads (25 MPa to 300 MPa) to achieve three different values of green density which were 57%, 67% and 78% of theoretical density, respectively in order to attain similar level of densification for both milled and as-received powder mixtures. To facilitate compaction and subsequent removal of the compacted samples, zinc-stearate powder was applied as die-wall lubricant.


**Fig. 3.3**: UTM 60 uniaxial semi-automatic hydraulic press

## 3.6 Design Modification of Microwave Furnace

The objective of design modification was to achieve ultra high vacuum (UHV) up to $10^{-5}$ mbar in the chamber, and thus to do sintering in non-oxidizing conditions. So the designs of parts were carried out using traditional methodology which was assisted by

modern analytical tools. An inexpensive modification brought the unit to use it in for what we aimed for.

The design of existing microwave furnace was initially based on its application at atmospheric pressure only. The inner chamber of furnace is made of 30×30×30 $cm^3$ stainless steel. The heaters, which are an assembly of rectangular-shaped waveguides and magnetrons (Figure 3.4), are clamped outside to it against two rectangular hollow-sections or windows on both sides of the furnace from where the electromagnetic waves enter into the chamber. Also, on top there's a circular hollow section on which IR pyrometer is suppose to be mounted for precision temperature measurement. A gas inlet is provided for application involving the use of an inert gas.

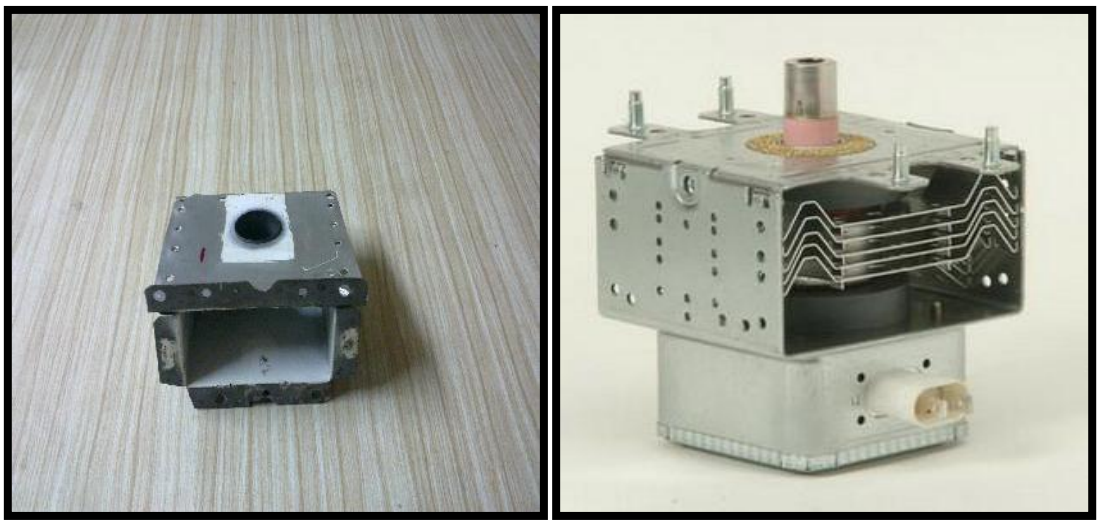

**Fig. 3.4**: Waveguide (left) and magnetron (right) used in microwave furnace.

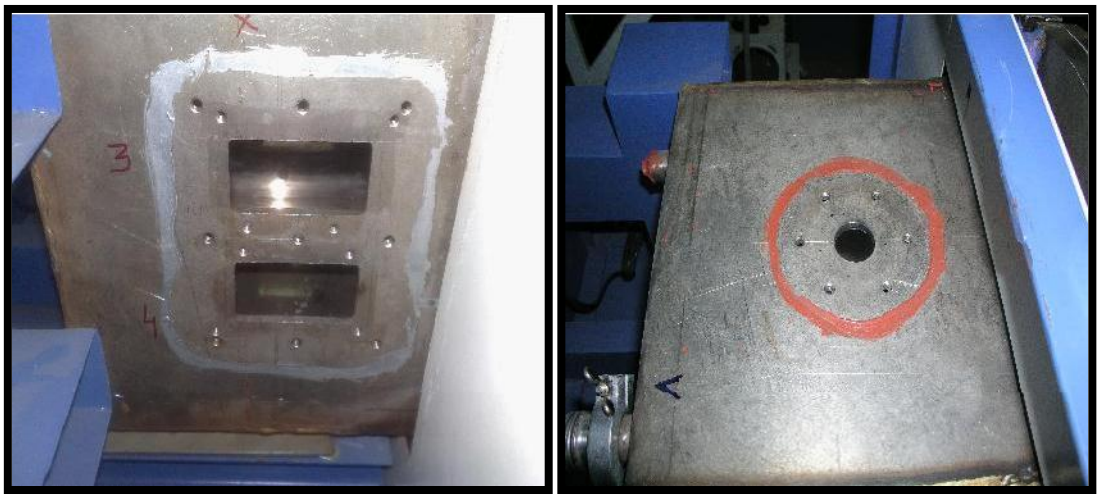

**Fig. 3.5**: Rectangular hollow sections on side (left) and circular hollow section on top (right) of microwave furnace

### 3.6.1 Design of Side Windows

For sealing rectangular windows present on the both sides of furnace chamber, design of two plates, namely seat plate and backing plate, were prepared using Solidworks 2007 (Figure 3.6). Both, seat plate and backing plate have two rectangular hollow section of exactly same size as that of windows on the furnace wall. The aim of having rectangular section on both the plates was to enable entrance of microwave energy into the chamber without any interference. Material chosen for both the plates was stainless steel. The seat plate has two O-ring grooves surrounding the hollow sections of it. Silicone rubber was chosen as O-ring material because of its exceptional heat and compression set resistance. Actual sealing was suppose to be done by an infrared grade fused-quartz glass plate, placed inside the seat-plate onto the O-rings and pressure is applied by backing plate which is joined to seat-plate by suitable screws. The selection of quartz plate was based on the fact that ait has low coefficient of thermal expansion, good strength and allows good transmission of microwaves with negligible reflection loss. The whole assembly (Figure 3.7) was welded on to the wall against the hollow section of the chamber such that backing plate, quartz glass and O-rings can removed whenever required.

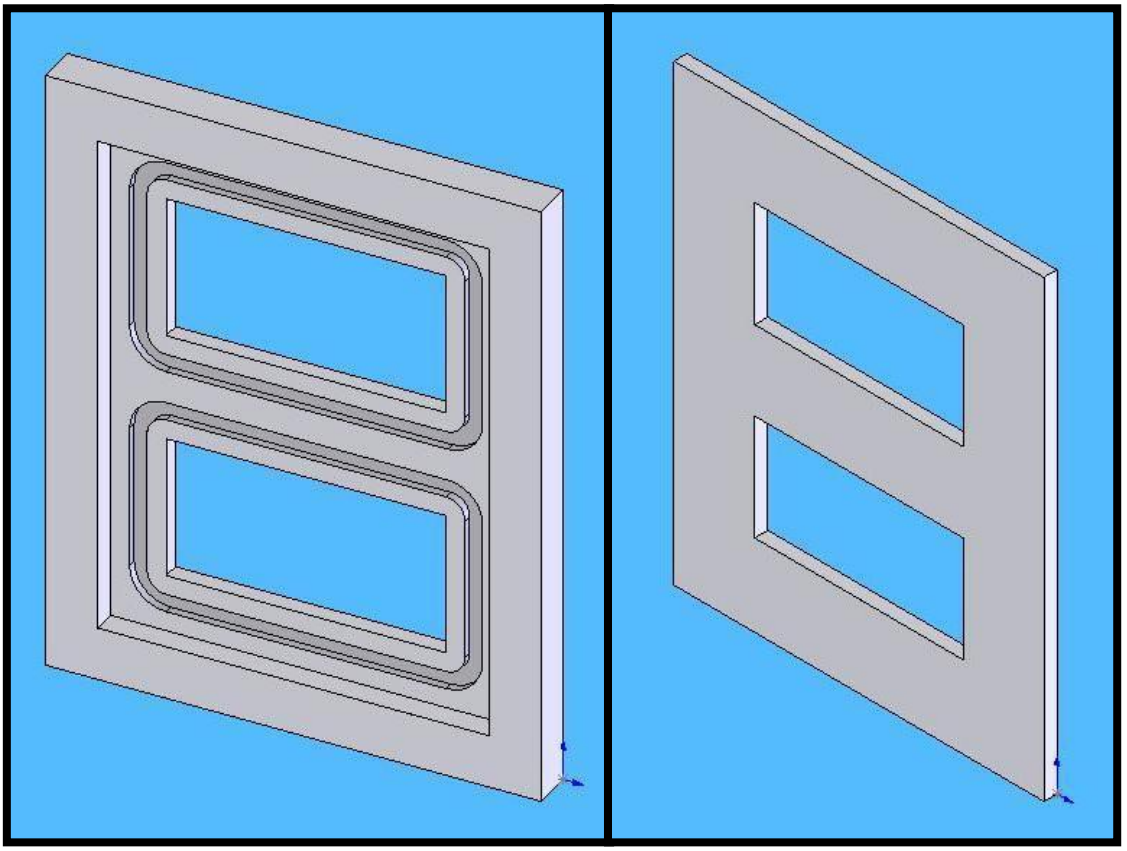

**Fig. 3.6**: SolidWorks part drawings for Seat Plate (left) and Backing Plate (right).

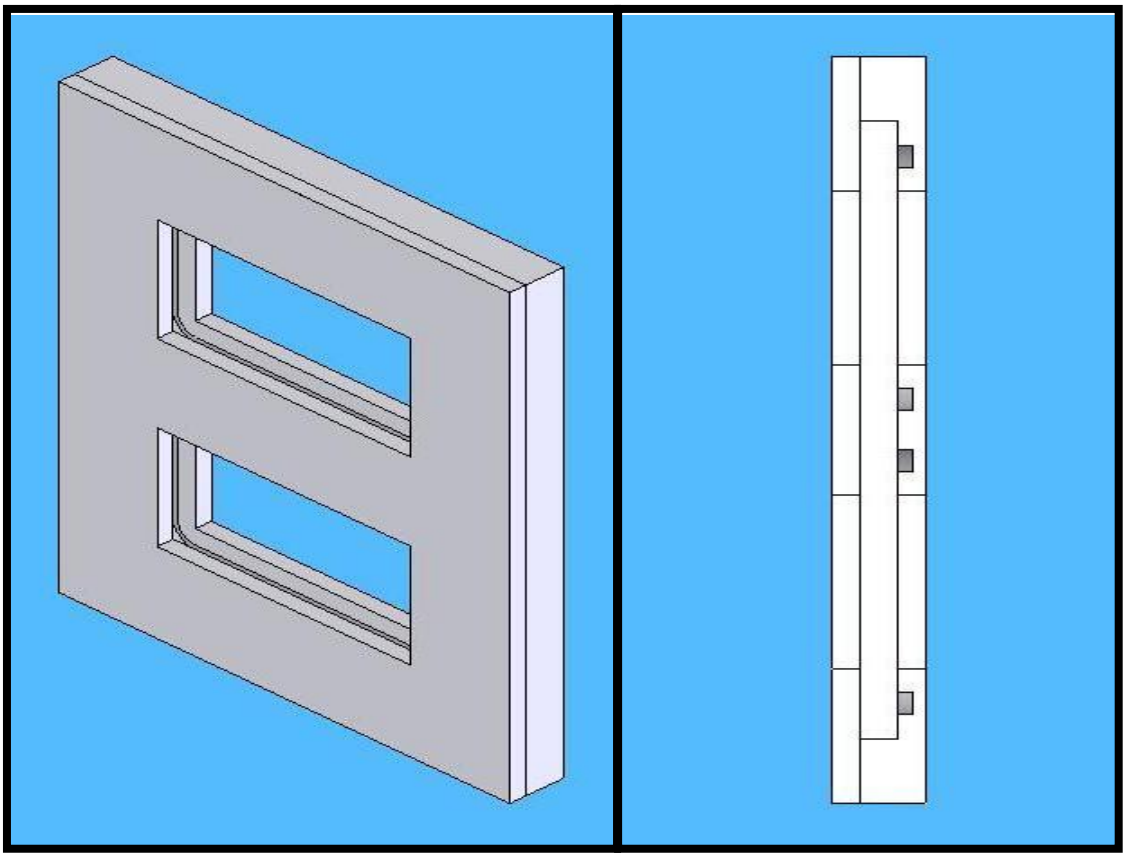

**Fig. 3.7**: Solidworks assembly drawings, isometric view (left) and sectioned side view (right), of Seat Plate and Backing Plate for side window.

### 3.6.2 Design of Top Window

For sealing top circular window, design of a disc and shaft were prepared using Solidworks 2007. The disc has a circular hollow section (Figure 3.8) matching with the hole on the top of furnace chamber such that application of infrared pyrometer could be possible and O-ring groove is provided around it. Also, disc has a seat on which glass is suppose to be sit which will provide compression to O-ring and thus sealing. Silicone rubber was chosen as o-ring material in this case also. Calcium Fluoride crystal was chosen as glass material because it has best transmission value (around 93%) for infrared waves such that accurate temperature measurements can be taken. The disc was made up of stainless steel and was welded to furnace top whose hollow section come about with that of furnace.

The shaft was so designed such that pyrometer could be mounted on to it vertically. The shaft has internal threads matching with external threads of pyrometer. The bottom end of the stainless steel shaft has flange of same size as that of disc and they

can fastened with screws such that glass and O-ring can be easily removed whenever required.

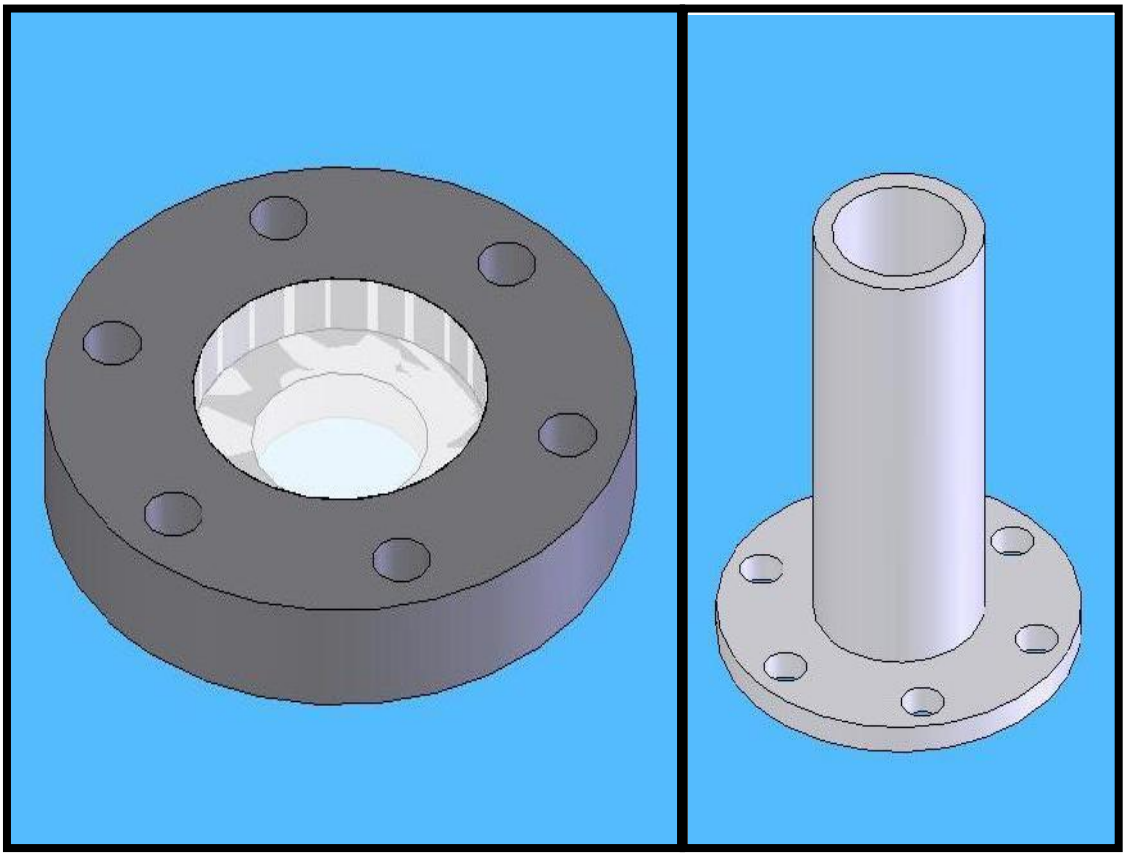

**Fig. 3.8**: Solidworks part drawing of disc (left) and shaft (right) for top window of microwave furnace.

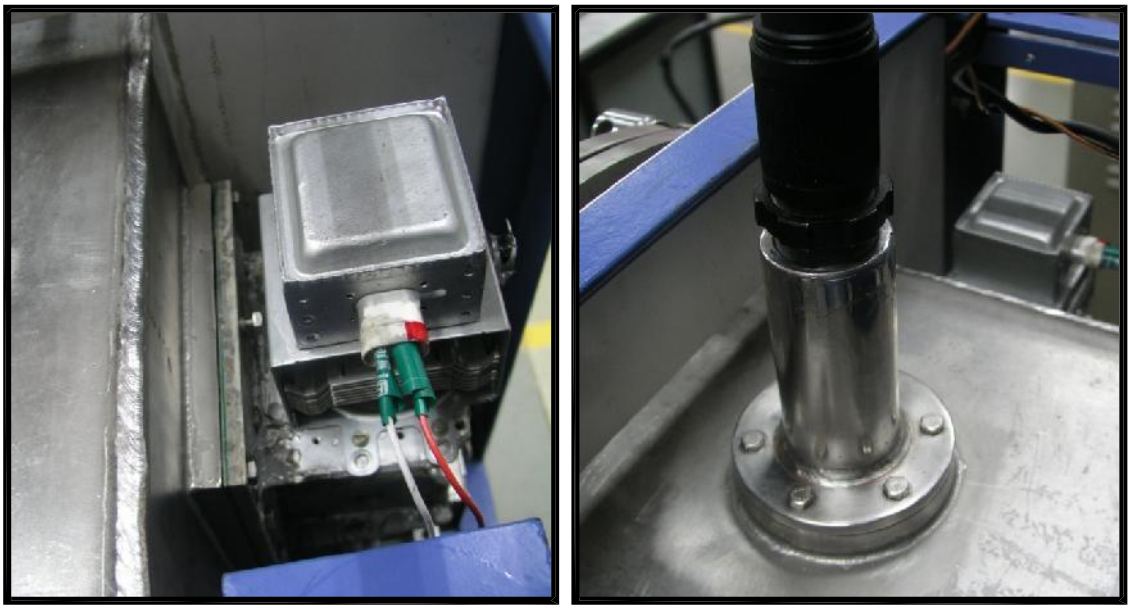

**Fig. 3.9**: Side Window assembly (left) and Top Window assembly (right) after modification of microwave furnace.

## 3.7 Sintering Procedure

The compacts were sintered by two consolidation techniques, microwave sintering and conventional sintering. The sintering of all compacts was carried out at 1050 °C for three soaking periods, i.e. 30 minutes, 60 minutes and 3 hours, under a flowing argon atmosphere. Table 3.2 shows variables chosen for the present study.

### 3.7.1 Microwave Sintering

Microwave sintering of green compacts was carried out using singlemode cavity 2.45 GHz, 1kW customized-built microwave furnace (Manufacturer: VB Ceramics, Chennai). It is equipped with high vacuum capability, as well as complete control for gas atmospheres.

A multi-layered insulation package was used to provide sufficient insulation to obtain high and uniform temperatures throughout the sample. The casket which was made by arrangement of zirca blocks from all sides, leaving a rectangular-shaped cavity, was covered by an outer layer of thick ceramic fiber wool.

**Table 3.2**: Summary of the experimental variables chosen for the present study.

| | | | Milling Hours | Green Density (%) | Soaking Time (mins) |
|---|---|---|---|---|---|
| 75Cu-25Cr | Sintering temperature 1050 °C | Microwave Sintering | 0 | 57 | 30 |
| | | | | | 60 |
| | | | | | 180 |
| | | | | 67 | 30 |
| | | | | | 60 |
| | | | | | 180 |
| | | | | 78 | 30 |
| | | | | | 60 |
| | | | | | 180 |
| | | | 9 | 57 | 30 |
| | | | | | 60 |
| | | | | | 180 |
| | | | | 67 | 30 |
| | | | | | 60 |
| | | | | | 180 |
| | | | | 78 | 30 |
| | | | | | 60 |
| | | | | | 180 |
| | | Conventional Sintering | 18 | 57 | 30 |
| | | | | | 60 |
| | | | | | 180 |
| | | | | 67 | 30 |
| | | | | | 60 |
| | | | | | 180 |
| | | | | 78 | 30 |
| | | | | | 60 |
| | | | | | 180 |

Inside the cavity, samples were placed over a thin plate of Cumilag 26 insulation brick and were surrounded by SiC plates used as susceptors from all four sides. The susceptors usually couple very well with the microwaves and are used for initially raising the temperature of the compact (Figure 3.11).

The sintering temperature selected for solid-phase sintering (SPS) was 1050 $^{\circ}$C at a heating rate of 50 $^{\circ}$C/min in an inert atmosphere of flowing argon gas. Three soaking times i.e. 30 min, 60 min and 180 min were provided at 1050 $^{\circ}$C. The temperature of the sample was monitored using an infrared pyrometer (Model: Raytek XRG5SF; manufacturer: Raytek Co., Santa Cruz, CA, USA). The pyrometer is emissivity based and usually emissivity varies with temperature. Temperature measurements for all compacts were done by using emissivity value of 0.95. This value was chosen based on sample color and composition. To verify the accuracy of selected value of emissivity changing with temperature, measurements were done for the same composition in a conventional furnace equipped with thermocouple simultaneously using infrared pyrometer.

**Fig 3.10**: Microwave furnace used for sintering Cu-Cr alloy

**Problem of Arcing**

During trial runs, arcing was observed inside the chamber immediately when the furnace was turned on. It was found that inside the chamber there was presence of sharp corners and edges especially at areas where microwave energy coming from waveguides enters inside the chamber. So, the rough surfaces and corners were grounded and smoothen well using suitable files.

Again after switching the furnace on, instead of occurring inside the chamber, arc was observed between two metal plates of side-window on both sides of the chamber. To restrain arc there, a solventless epoxy resin called Bisphenol A diglycidyl ether (BADGE) mixed with diethyle triamine (DETA) used as hardner in a ratio of 8.5:1 was applied on the meeting surface of metal plates. Fortunately afterwards, there was no sign of arc between metal plates. The compound we used has good dielectric strength, act as a capacitor, which prevented arcing between the plates.

**Fig 3.11**: Loading of green compact in a insulation package used for microwave furnace

But while on running experiment with no susceptors used, arcing was observed inside the cavity of casket around the samples and consequently furnace was turned off. This may have occurred because extremely high field must have existed in the cavity of the casket. So when the fours susceptors were placed inside the cavity around the sample, the arcing didn't occur because it absorbs majority of incident power and convert it to heat. SiC susceptor plates used, being high lossy material, have thickness equal to 1.1

cm which is more than the penetration depth which is equal to 0.8 cm at 2.45 GHz which eventually reduces the field strength inside the chamber. As a result, arcing got eliminated and from that point onwards experimentation got started.

### 3.7.2 Conventional Sintering

The conventional sintering of green compacts was carried out in a high temperature graphite furnace (Manufacturer: Therelek Engineers, Bangalore) at a constant heating rate of 10 $^{\circ}$C/min. Final temperature and soaking times for conventional sintering are same as that of microwave sintering. Samples were loaded in a graphite crucible (Figure 3.12) and heating was also done in an inert atmosphere of flowing argon.

**Fig. 3.12**: Conventional high temperature graphite furnace

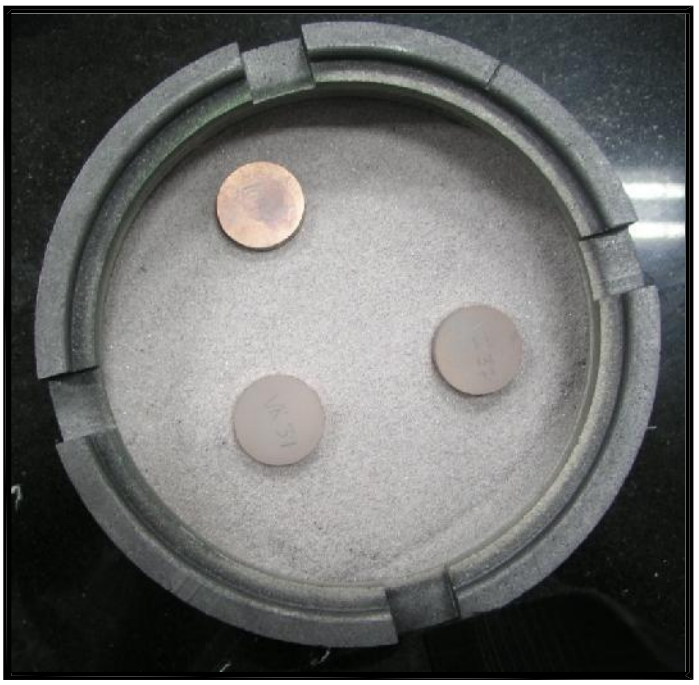

**Fig. 3.13**: Loading of green compacts in graphite crucible used for conventional furnace.

## 3.8 Characterization and Testing of Sintered Specimens

### 3.8.1 Microstructural Investigation

The sintered samples were mounted with the help of epoxy and wet polished in a manual polisher (model: Lunn Major, supplier: Struers, Denmark) using a series of SiC papers, followed cloth polishing using a suspension of 1 μm, 0.3 μm, and 0.05 μm alumina. An optical microscope with digital image acquisition capability (model: Olympus BX series) was used to obtain the micrographs of sintered samples. The photographs of representative regions were taken at appropriate magnifications.

A scanning electron microscope (model: Quanta 200, supplier: FEI, USA) was used for the morphology, particle size and microstructural characterization of different sintered specimens. Micrographs are taken at suitable accelerating voltages for the best possible resolution using the secondary electron imaging.

### 3.8.2 Sintered Density

Densities of the sintered cylindrical pellets were calculated from the mass and physical dimension measurements on the sample. The density was also reconfirmed by Archimedes water displacement method.

### 3.8.3 Microhardness

Microhardness tester (model: LM 300 AT, supplier: Leco, USA) was used to determine Vickers hardness values of all the sintered specimens using 0.5 kg load for a dwell time of 10 s. Five readings were taken for each specimen.


**Fig. 3.14**: Leco LM 300 AT hardness tester

### 3.8.4 Electrical Conductivity

The electrical conductivity of all the sintered samples was investigated by 4-probe method in SIGMATEST D 2.068, FOERSTER instrument. The conductivity was as per the International Annealed Copper Standard (IACS) (100%).

# Chapter 4 Results and Discussion

## 4.1 Characterization of Milled Powder

### 4.1.1 Particle Size and Surface Area Analysis

The particle size and size distribution analysis of milled and as-received powders are summarized in Table 4.1. It is clear from the table 4.1 that as-received powder is distributed over wide range than both 9 hour-milled and 18 hour-milled powder. Also, there is not much difference in size distribution of 9 hour-milled and 18 hour-milled powder. Due to mechanical milling of powder, the Sauter Mean Diameter (SMD) has considerably reduced to 87 % by 9 hours of milling and 86 % by 18 hours of milling. The reduction in particle size has been observed maximum in 9 hours milled powder. Particle size for 18 hours milled powder is almost same as that of 9 hours. It seems at this stage the rate of fracturing might be equal to rate of welding where no change in particle size takes place. Fig. 4.1 shows the particle size distribution curve for as-received, 9 hour-milled and 18 hour-milled chromium powder. As seen from the figures there is lot of difference in the distribution curve for as-received and milled powder where curve for 9 hours-milled and 18-hours milled is similar.

**Table 4.1**: Size and surface area of as-received and milled chromium powders

| **Property** | | **As-received** | **9 hr milled** | **18 hr milled** |
|---|---|---|---|---|
| **Particle size (µm)** | $\mathbf{D_{10}}$ | 9.58 | 1.10 | 1.23 |
| | $\mathbf{D_{50}}$ | 26.44 | 3.85 | 4.09 |
| | $\mathbf{D_{90}}$ | 51.25 | 8.67 | 8.91 |
| **SMD (3,2) (µm)** | | 17.81 | 2.17 | 2.4 |
| **BET Surface Area ($m^2/g$)** | | 0.62 | 1.32 | 0.96 |
| **Specific Surface Area ($m^2/m^3$)** | | 336.71 | 2757.23 | 2498.45 |
| **Apparent Density ($g/cm^3$)** | | 2.48 | 1.92 | 2.08 |

Also, referring to Table 4.1, adsorption surface area of 9 hour-milled powder has maximum value in comparison to as-received and 18 hour-milled chromium powder. The adsorption surface area of 9 hour-milled powder is almost half of that of powder in as-received condition. The reason for increase in value of surface area could be that powder has irregular shaped with high degree of roughness or it could be that powder has finer particle size. The as-received powder has flaky-shaped structure and a

coarser particle size and wider particle size distribution which make it having low surface area. The milled powder should have round morphology with finer particle

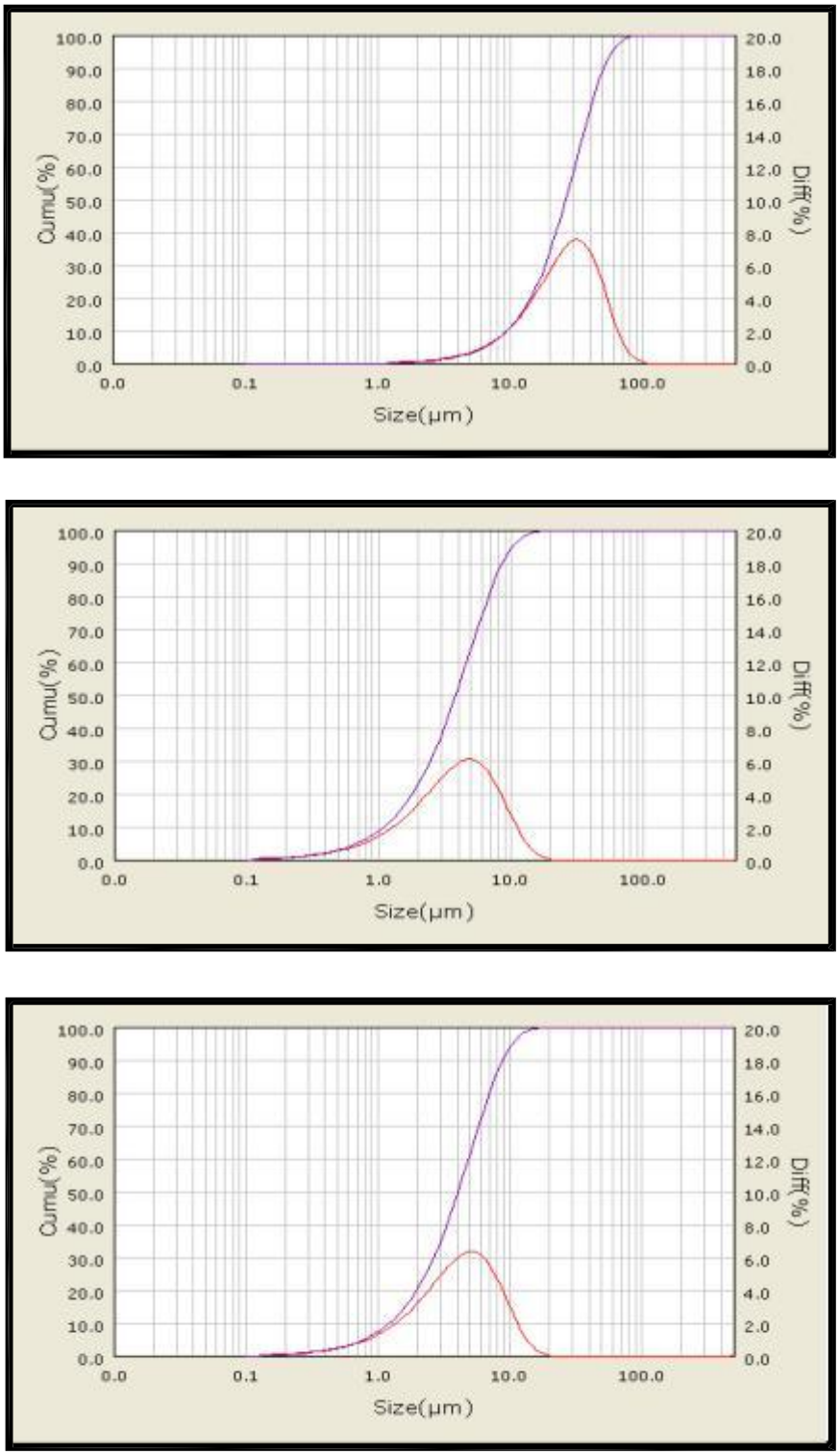


**Fig. 4.1**: Particle size distribution curve for as-received, 9 hour-milled and 18 hour-milled chromium powder, respectively.

size and narrow particle size distribution in comparison to as-received powder which might accounts for its high surface area.

The value of apparent density is least in case of 9 hour-milled powder. Particle size and shape, surface area and its distribution are characteristics which have direct bearing on apparent density. As the surface area has increased for milled powder it indicates the increase in particle-particle friction, known as internal friction, and friction between particle and wall of container, known as external friction. But due to milling particles have become fine which should have opposite effect. Also, particle size distribution of 9 hour-milled powder is narrow as compared to as-received powder which concludes that 9-hours milled will not have good arrangement and thus less apparent density.

To understand the effect of mechanical milling, structural characterization of the mechanically milled powder samples were carried out by SEM and XRD.

### 4.1.2 SEM Analysis

The micrographs of powder samples were taken using (FEI Quanta 200) scanning electron microscope in a Large Field Detector (LFD) mode. SEM micrographs in Fig. 4.2(a-c) show refinement of ball milled chromium powder. As- received powder has irregular and fluffy type of structure which when undergoes mechanical milling the morphology of powder has been changed to round. Spherical particles of milled powder also appear to be smooth. It is clearly distinguishable from SEM micrographs that particle size of 9 hour-milled powder is somewhat less than that of 18 hour milled powder. However, there is no difference in morphology between 9 hour-milled and 18 hour-milled powder. But in case of 18 hour-milled powder, the sub-micron sized particles seemed to be agglomerated more as compared to 9 hour-milled.

To know the contamination level in powder samples EDS analysis was carried out. EDS analysis revealed that with the increase in milling time contamination of iron in powder is increasing. EDS analysis curve for as-received, 9 hours-milled and 18 hours-milled are shown in the Figure 4.3 and 4.5, respectively. Presence of iron contaminants was probably due to impact of grinding medium on inner wall of hardened steel container used for our study. EDS analysis results are summarized in Table 4.2.

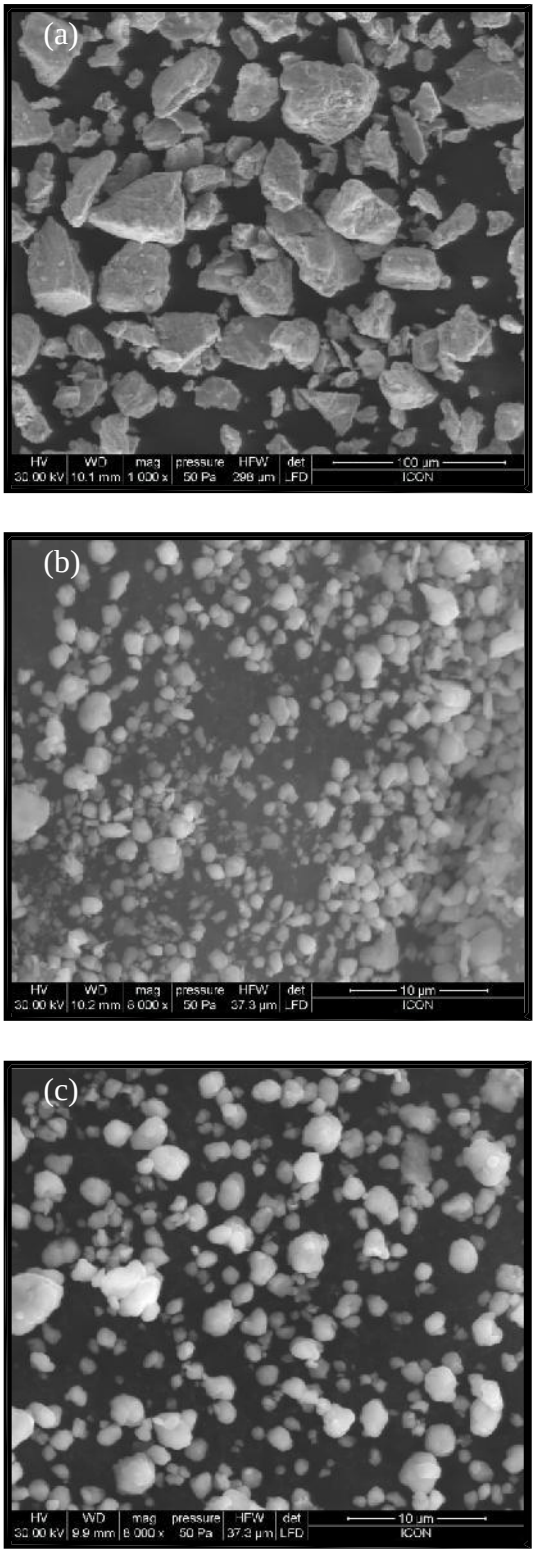


**Fig. 4.2**: SEM micrographs of (a) as-received, (b) 9 hour-milled and (c) 18 hour-milled chromium powder.

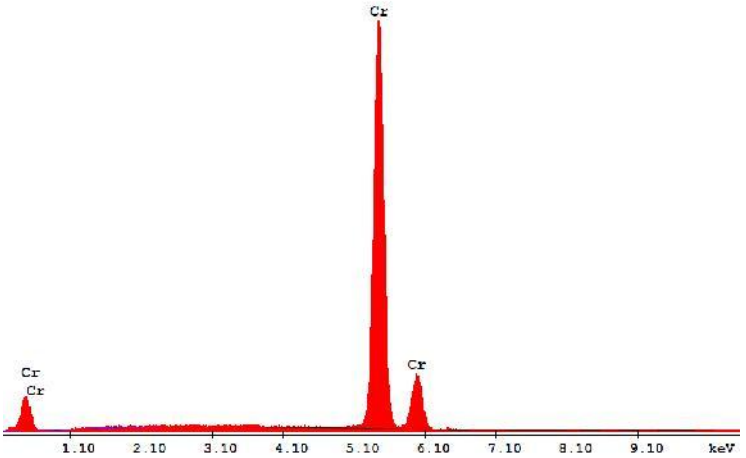


**Fig. 4.3**: EDS analysis of as-received chromium powder

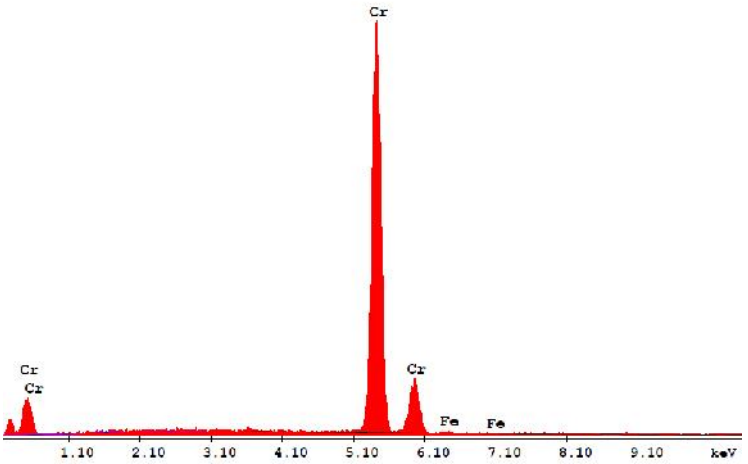


**Fig. 4.4**: EDS analysis of 9 hour milled chromium powder

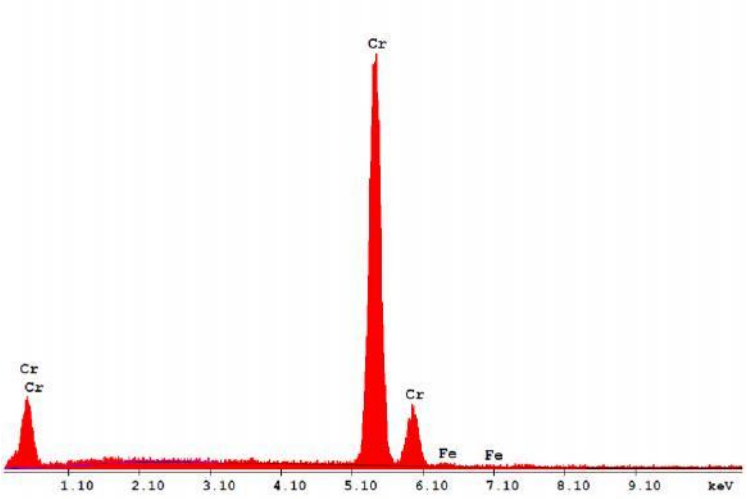


**Fig. 4.5**: EDS analysis of 18 hour milled chromium powder

**Table 4.2**: Results of EDS Analysis

| Powder | Element- Wt % | |
|---|---|---|
| | CrK | FeK |
| **As-received** | 100 | 0.0 |
| **9 Hour Milled** | 99.44 | 0.56 |
| **18 Hour Milled** | 98.67 | 1.33 |

### 4.1.3 XRD Analysis

Figure 4.6 shows XRD patterns of as-received and milled powder sample milled in WC grinding media. From the phase analysis it has been found that peak intensity much reduced from initial, without milled powder and peak broadening occur. A few small peaks corresponding to Fe, C and $Fe_3C$ phases were detectable from the 18 hour-milled. The carbon contamination was occurred possibly due to from toluene, which was used as a process control agent during milling. In case of 9 hour-milled powder, a few small peaks corresponds to Fe are visible along with the peaks of C. The peaks corresponding to Fe are due to the contamination from milling container.

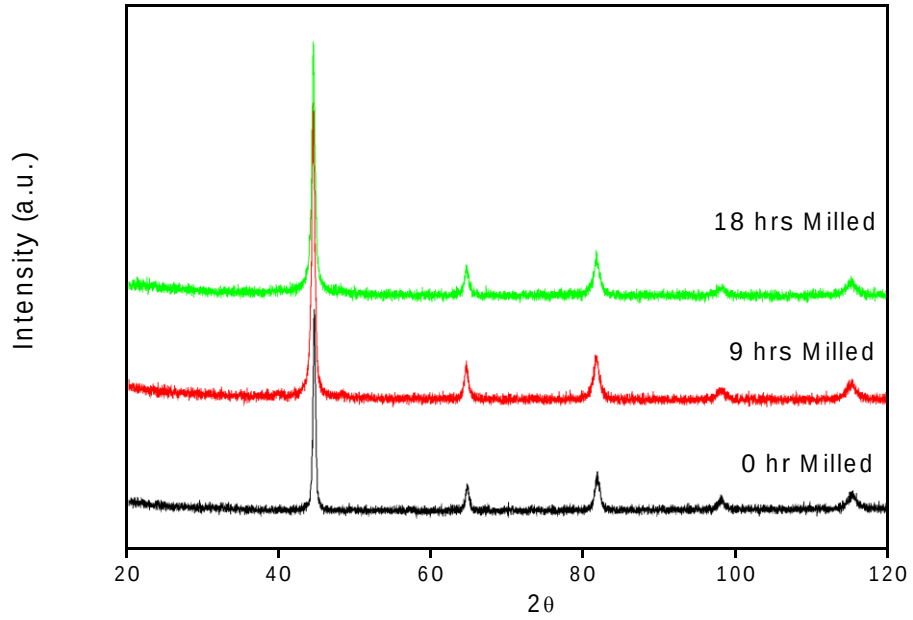


**Fig. 4.6**: XRD Analysis peaks for as-received, 9 hour milled and 18 hour milled chromium powder.

From XRD analysis, Cr peaks are visible from initial stage to 18 hours of milling. The broadening of peak and decrease in peak intensity are maximum for 18 hour-milled powder.

The crystallite size of powders was calculated from the half-height width of the diffraction peak of XRD pattern using the Debye-Scherrer equation. Analysis of the XRD data revealed that average crystallite size decreases from 34 nm of as-received powder to 23 nm of the milled powder where no change in crystallite size took place from 9 hours to 18 hours of milling.

## 4.2 Characterization of Sintered Samples

### 4.2.1 Heating Response

Fig. 4.7 shows the typical temperature-time profile of both microwave and conventional sintering at 1050$^{\circ}$ C for 30 min as peak-soaking period. It is evident from the figure that Cu-Cr alloy couple with microwaves and undergo rapid heating. In case of conventional furnace, in order to ensure uniform heating, the compacts heating rate was restricted to 10$^{\circ}$ C/ min and isothermal hold were provided at 650$^{\circ}$ C for 5 min in both the cases. In contrast, the overall heating rate in microwave furnace was up to 50$^{\circ}$ C/ min, much higher than that of conventional sintering. Getting rid of cooling periods in both sintering, there is about 75 % reduction in process time during microwave sintering.

### 4.2.2 Microstructural Investigation of Sintered Samples

The microstructural features of conventional and microwave sintered specimens were characterized by Optical Microscope and SEM. Figures 4.8 and 4.9 show the microstructures of solid phase sintered Cu-Cr alloys where compacted at different pressure; consolidated by conventional as well as microwave technique at 1050$^{\circ}$ C for 180 minutes soaking period. Figure 4.8 represents microstructures of compacts with as-received chromium powder whereas figure 4.9 represents microstructures of compacts with 9 hour-milled chromium powder. It is evident from both figures that there is a lot of difference in microstructures obtained from conventional and microwave conditions.

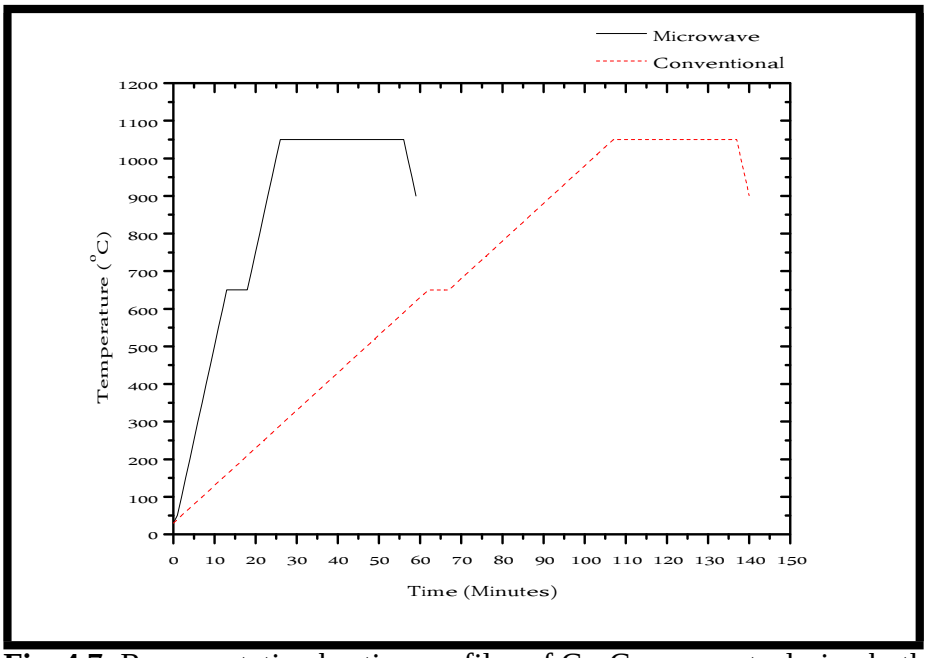


**Fig. 4.7**: Representative heating profiles of Cu-Cr compacts during both microwave and conventional sintering.

One significant difference between microwave and conventionally sintered samples is that in the former there is hardly any Cr grain growth, which is observed in the conventionally sintered Cu-Cr samples. Clearly, microwave sintering results in significantly lower Cr grain coarsening. Also, the distribution of chromium is finer in the microwave-sintered sample suggesting better mechanical properties. The most striking difference observed is that microwave sintering produces well rounded and finer chromium particles well separated from each other as opposed to the sharp, irregular and wedge shaped chromium particles for the conventionally-sintered samples. As particle shape becomes irregular, the number of contacts between particles increases which in turn decreases separation between the particles. However, the total porosity levels in both the cases appear to be more or less equivalent.

As seen from the figures, a lot of difference in microstructures is observed between compacts made out of as-received chromium powder and those of milled chromium powder consolidated by both conventional and microwave technique. Cr phase is more rounded and finer in case of microwave consolidated compacts with milled chromium powder as compared with the non-separated irregular shaped Cr particles observed for conventionally sintered sample with milled chromium powder.

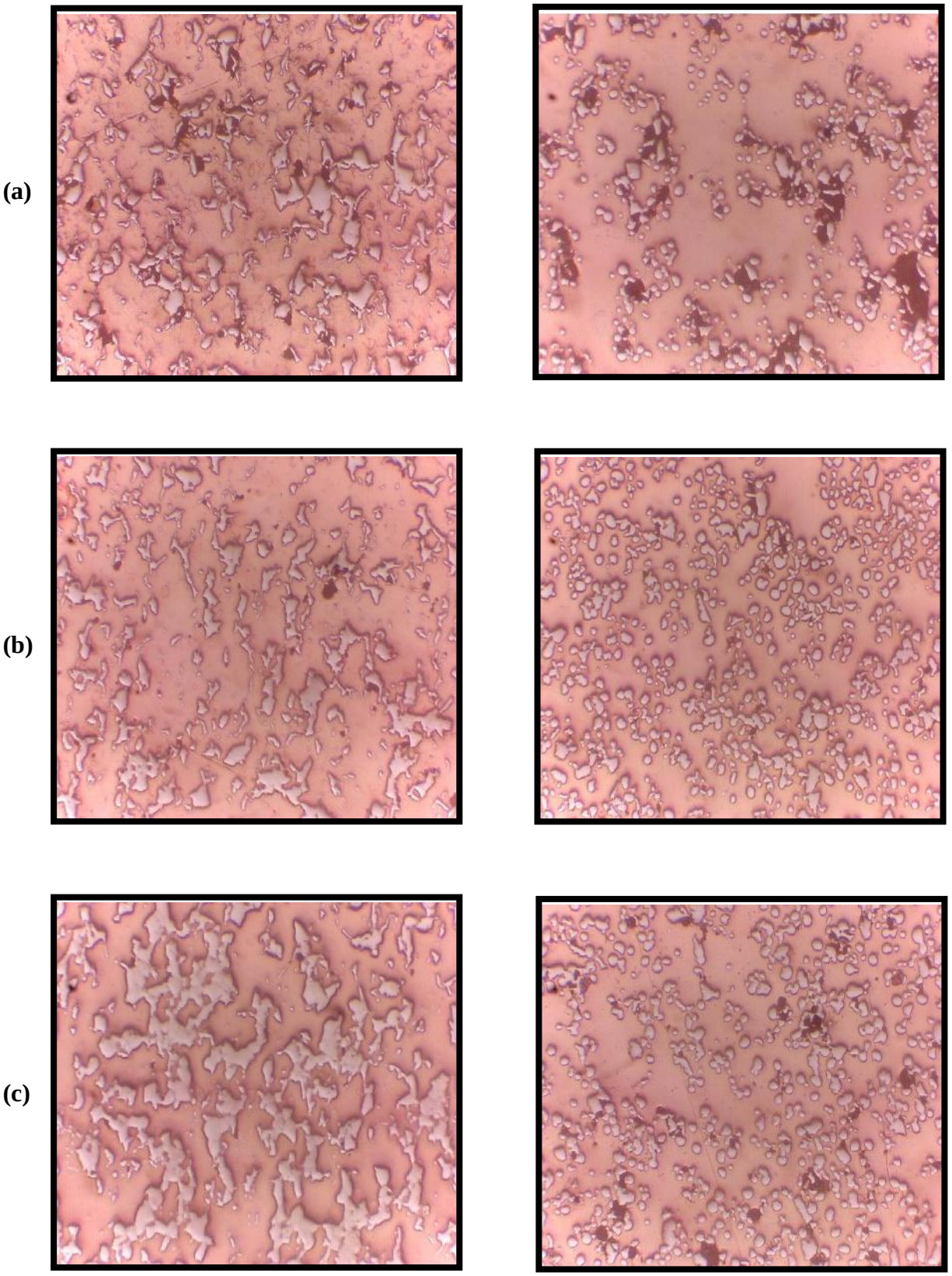


**Fig. 4.8**: Microstructure of Cu-25Cr alloy with as-received Cr compacted at (a) 57% (b) 67% and (c) 78% green density value and sintered by Conventional (left) and microwave (right) technique for 180 minutes.

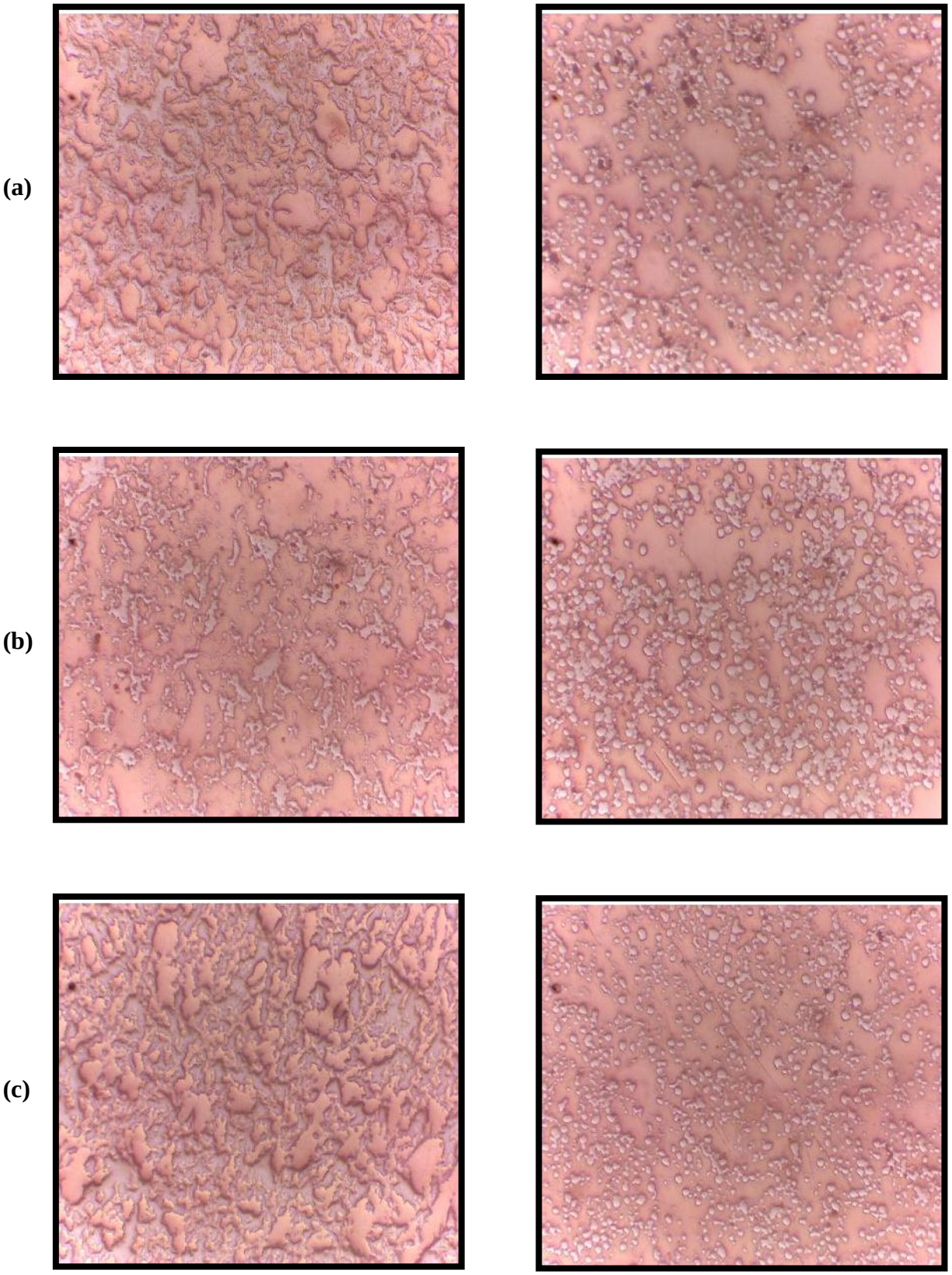


**Fig. 4.9**: Microstructure of Cu-25Cr alloy with 9-hour milled Cr compacted at (a) 57% (b) 67% and (c) 78% green density value and sintered by conventional (left) and microwave (right) technique for 180 minutes.

**SEM analysis of sintered samples**

The microstructures of polished sintered samples were taken using (FEI Quanta 200) scanning electron microscope in black scattered image mode. Figure 4.10 (a-d) compare the microstructures of Cu-75Cr alloy sintered at 1050° C for 180 minutes by conventional and microwave techniques. Clearly, microwave sintered samples showed more roundness of Cr particles and significantly lower grain coarsening than that of conventionally sintered specimens. Better grain distribution and uniform grain size with less porosity in microwave sintered specimen is expected to provide better combination of mechanical property like hardness and electrical conductivity.

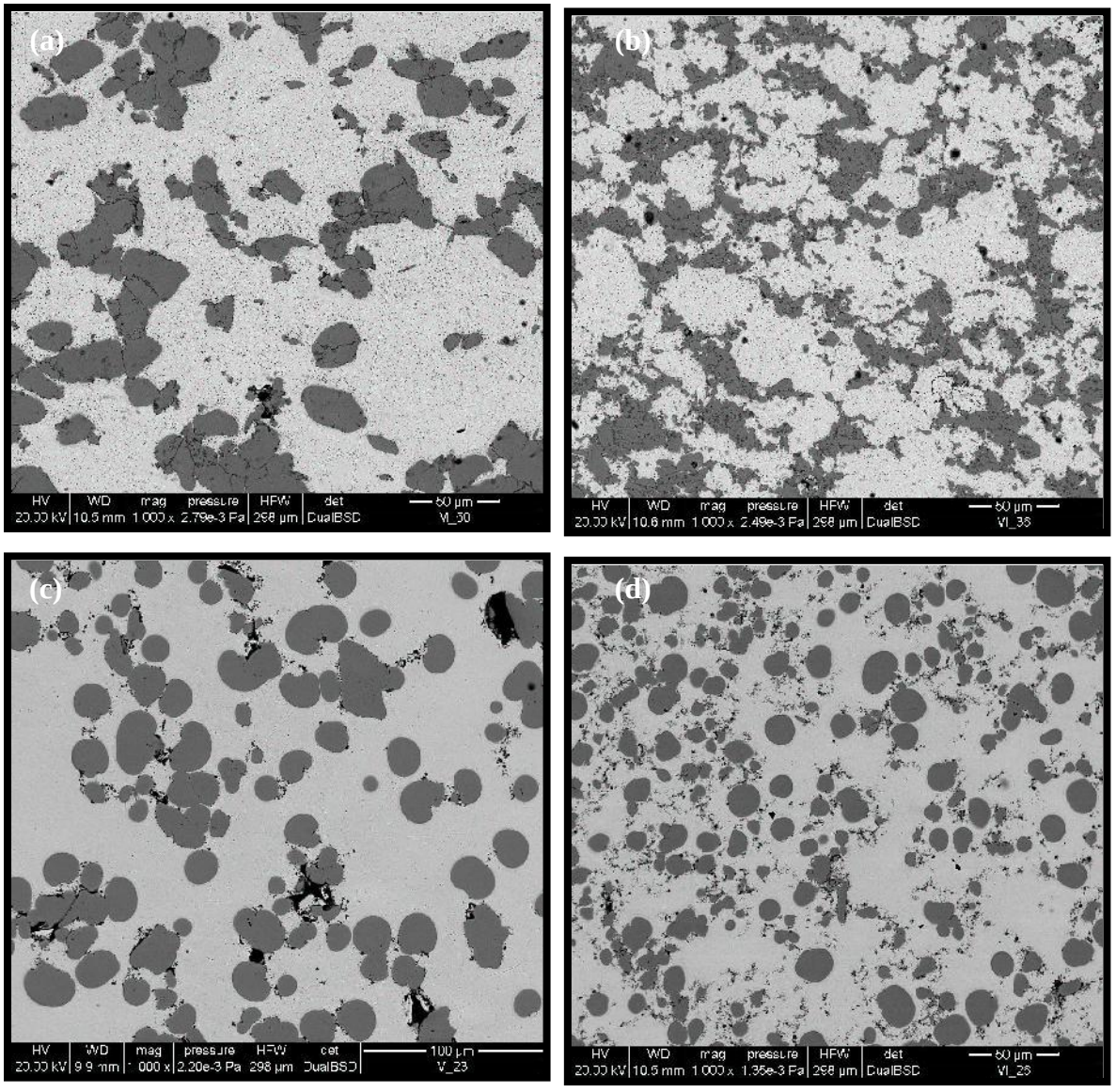


**Fig. 4.10**: SEM micrographs of conventionally sintered ((a),(b)) and microwave sintered ((c),(d)) with as-received (left) and 9-hour milled powder (right) chromium powder at 1050° C for 180 minutes.

It is evident from the figure 4.10 ((b) and (d)) with combined effect of mechanical milling and microwave grains have become more uniform and rounded morphology as compared to conventional sintered specimen with milled powder having irregular morphology. It is clear from the figure that connectivity and contiguity of Cr particles is lowest for microwave sintered specimen with milled Cr particle than its conventional counterpart where the segregation of chromium in copper phase appears to be more.

### 4.2.3 Evaluation of Density

Density values determined using Archimedes principle are tabulated in Table 4.3. The maximum densification in conventionally sintered compacts is around 85% of theoretical density whereas sintered compacts by microwave technique shows significantly higher densification, about 92% of theoretical density. It is clear from the table that, compacts with higher green density resulted in higher percentage densification. The overall enhancement in sintered density by microwave technique is about 6.3% more than conventionally sintered compacts.

**Table 4.3**: Relative sintered densities of Cu-Cr compacts with green density values as 57%, 67% and 78% of TD, conventionally and microwave sintered at 1050$^{\circ}$C and each soaked for 30 minutes, 60 minutes and 180 minutes.

| **Green Density Value = 57 % of TD** | | | | | | |
|---|---|---|---|---|---|---|
| **Peak Soaking Time (mins)** | **Conventional** | | | **Microwave** | | |
| | **As-received** | **9 Hr Milled** | **18 Hr Milled** | **As-received** | **9 Hr Milled** | **18 Hr Milled** |
| **30** | 66.1 | 67.8 | 66.0 | 72.5 | 63.9 | 81.0 |
| **60** | 67.4 | 68.8 | 68.0 | 83.5 | 77.3 | 67.8 |
| **180** | 66.9 | 69.2 | 68.4 | 70.8 | 67.5 | 73.4 |
| **Green Density Value = 67 % of TD** | | | | | | |
| **Peak Soaking Time (mins)** | **Conventional** | | | **Microwave** | | |
| | **As-received** | **9 Hr Milled** | **18 Hr Milled** | **As-received** | **9 Hr Milled** | **18 Hr Milled** |
| **30** | 75.8 | 76.7 | 76.3 | 84.9 | 82.6 | 79.6 |
| **60** | 79.2 | 76.9 | 75.7 | 86.7 | 84.3 | 82.9 |
| **180** | 77.7 | 75.3 | 76.0 | 80.6 | 82.2 | 81.4 |
| **Green Density Value = 78 % of TD** | | | | | | |
| **Peak Soaking Time (mins)** | **Conventional** | | | **Microwave** | | |
| | **As-received** | **9 Hr Milled** | **18 Hr Milled** | **As-received** | **9 Hr Milled** | **18 Hr Milled** |
| **30** | 84.2 | 84.8 | 82.9 | 84.7 | 85.3 | 90.9 |
| **60** | 85.3 | 85.4 | 84.2 | 89.4 | 92.1 | 90.8 |
| **180** | 84.6 | 85.5 | 85.1 | 87.7 | 85.0 | 89.7 |

In some cases, only for microwave sintered compacts with lowest relative green density compacts, Cu melt exudation took place. Cu exudation is an undesirable problem and badly deteriorates the composition retention and microstructural homogeneity [47,48]. With the exception such few cases, microwave sintering results in better densification. Since factors that contribute to enhanced diffusivity are known to enhance densification during sintering, it can be inferred that the atomic transport is higher in case of microwave sintering [49].

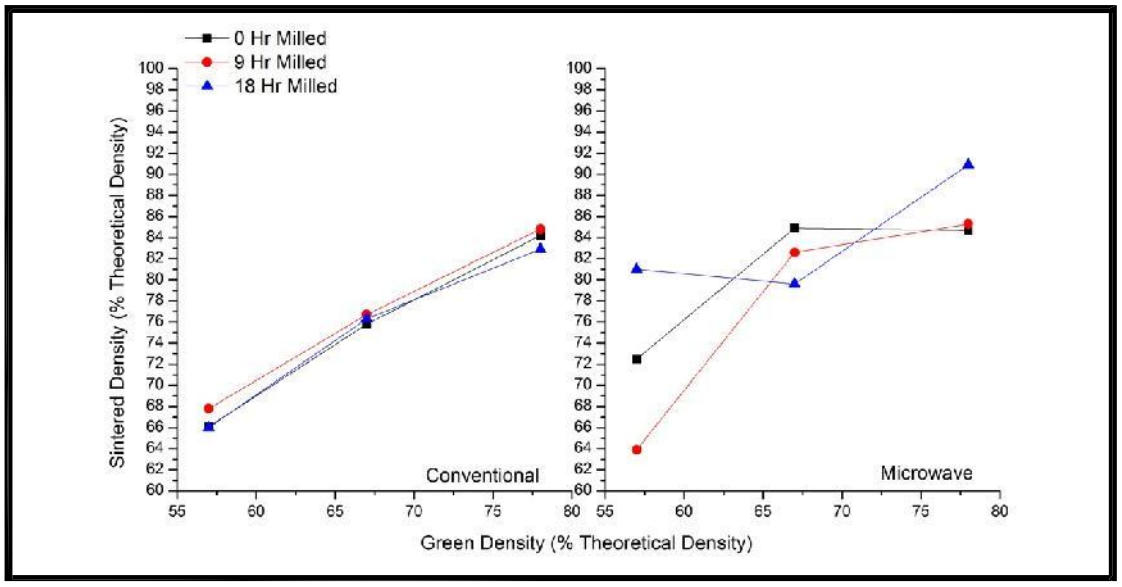


**Fig. 4.11**: Variation of relative sintered density with green density for compacts soaked at 1050° C for 30 mins in conventional and microwave furnace.

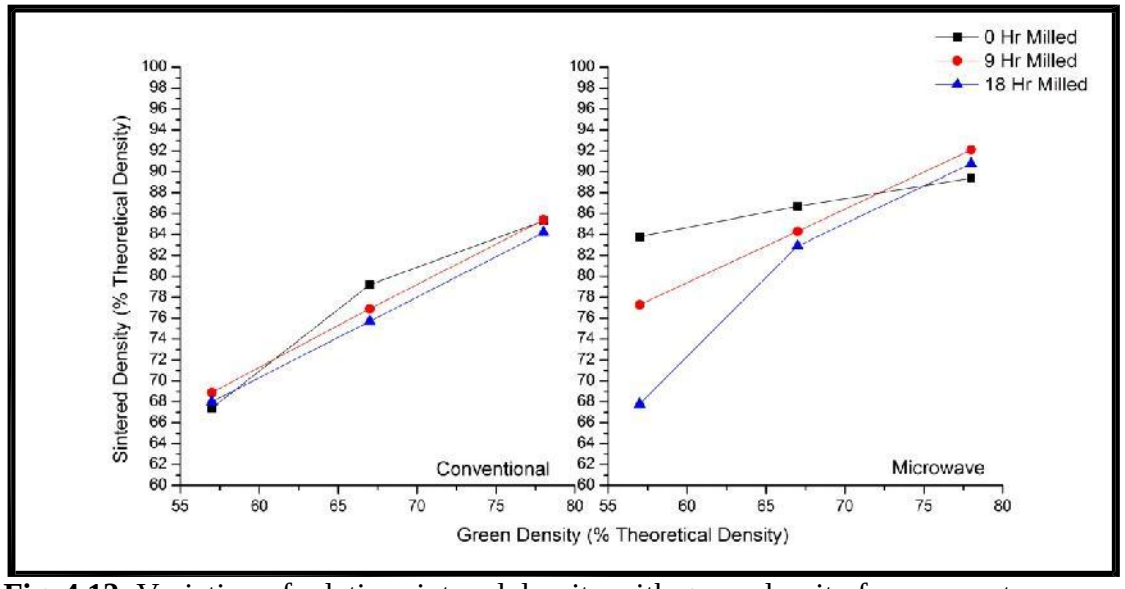


**Fig. 4.12**: Variation of relative sintered density with green density for compacts soaked at 1050° C for 60 mins in conventional and microwave furnace.

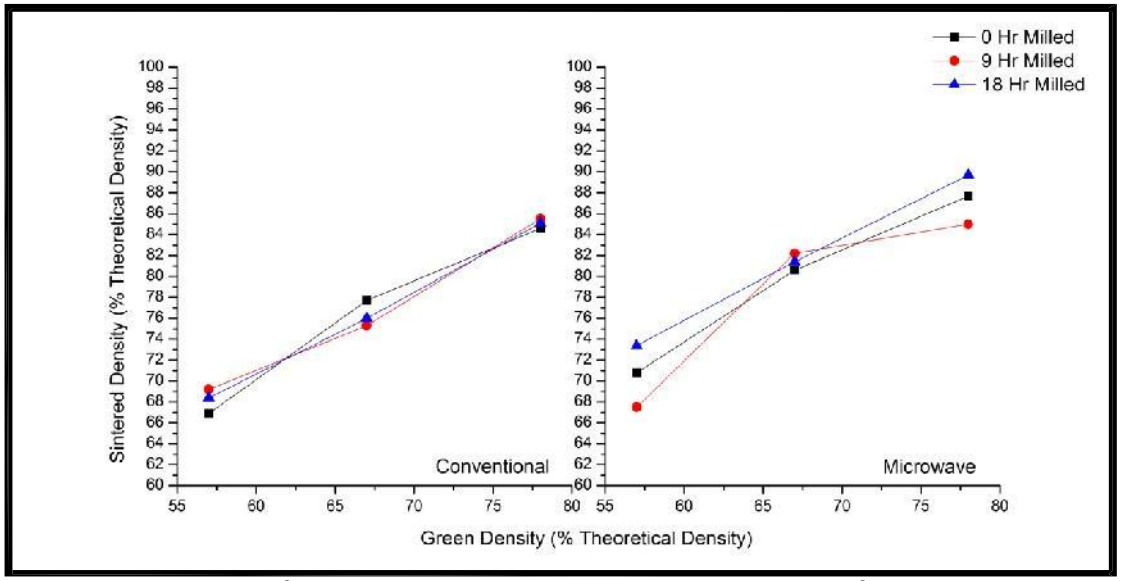


**Fig. 4.13**: Variation of relative sintered density with green density for compacts soaked at 1050° C for 180 mins in conventional and microwave furnace.

It is clearly evident from the figure 4.11 to 4.13 all compacts show improvement in sintered density with increasing relative green density. When the powder is compacted to higher pressure, the number of contacts it makes with neighboring particles is more. This increases the interfacial area between the particles, which hastens diffusion kinetics.

Longer soaking time is beneficial to the densification because the solid-phase sintering of the skeleton is a diffusion-controlled process [50]. Therefore, the sintered density of Cu-25Cr should increase with soaking time. However, from figure 4.14 to 4.16 we note that higher soaking time didn't result in the expected increase.

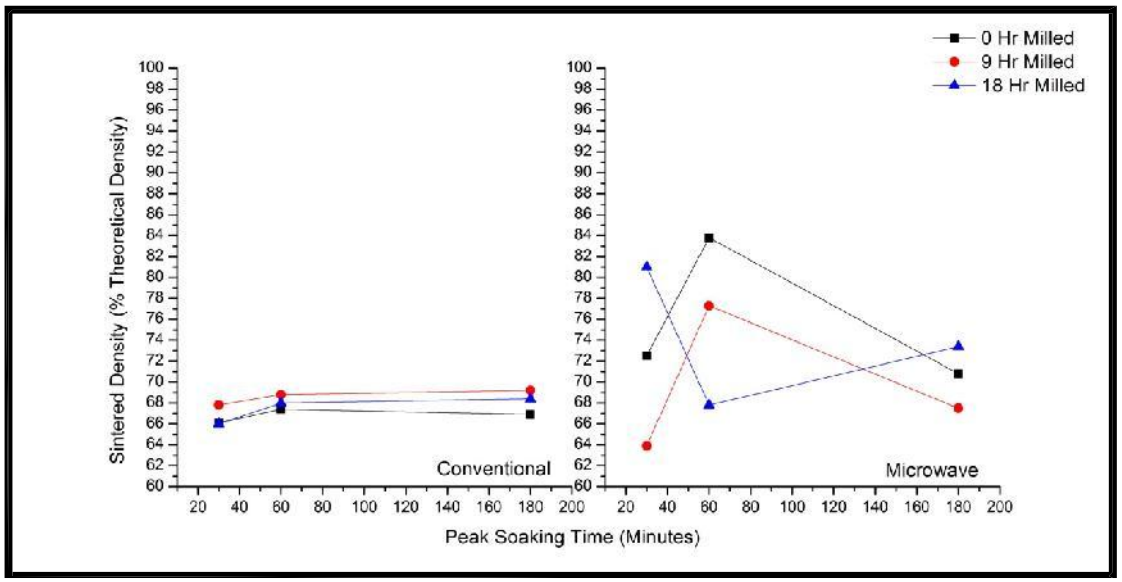


**Fig. 4.14**: Variation of relative sintered density with soaking time for compacts with green density 57 % of TD sintered in conventional and microwave furnace.

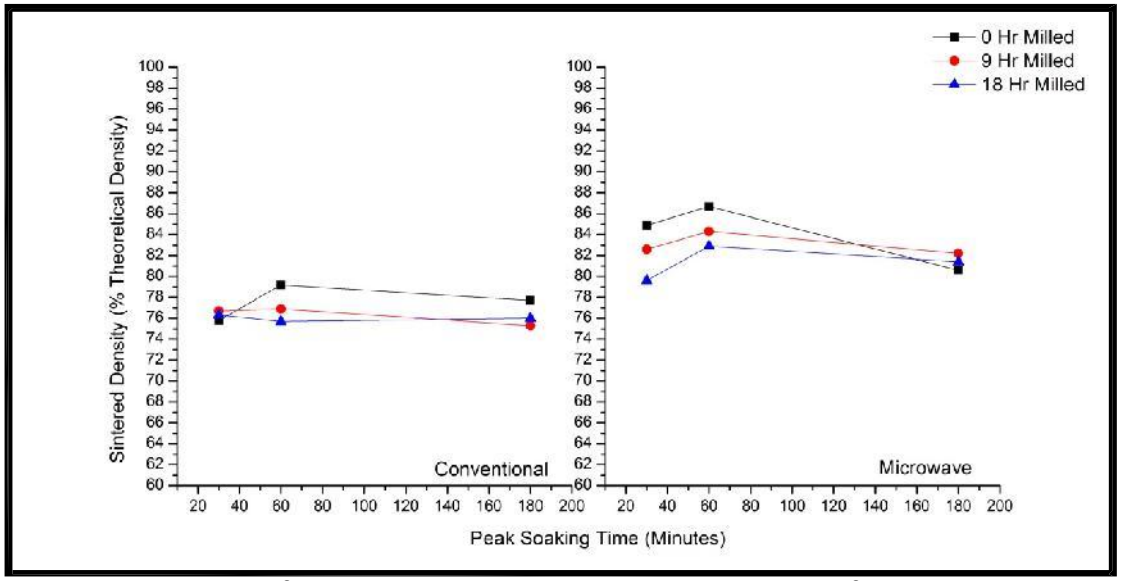


**Fig. 4.15**: Variation of relative sintered density with soaking time for compacts with green density % of TD sintered in conventional and microwave furnace.

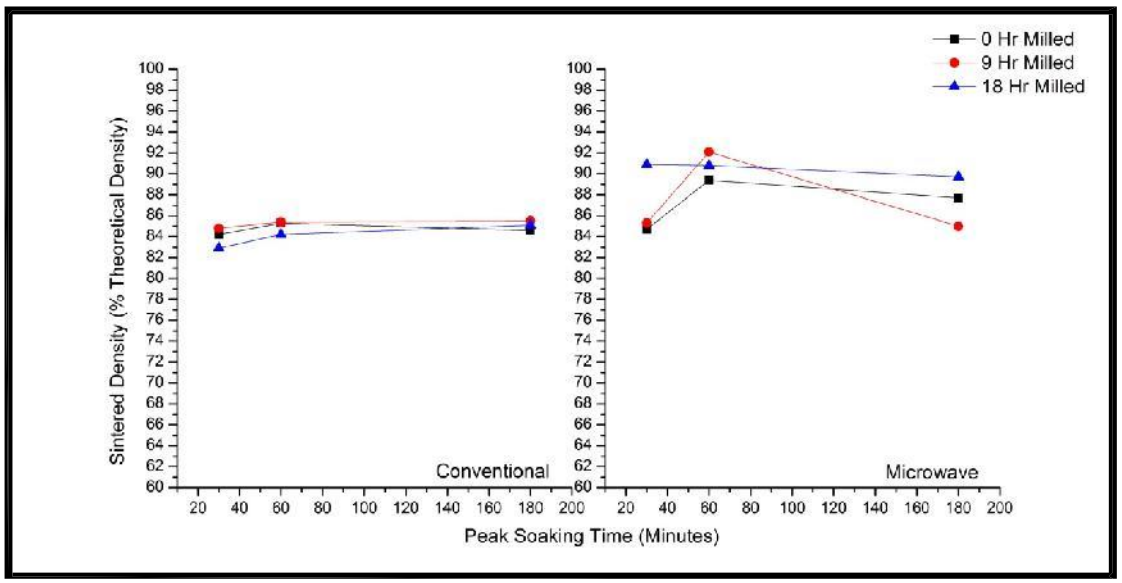


**Fig. 4.16**: Variation of relative sintered density with soaking time for compacts with green density 78 % of TD sintered in conventional and microwave furnace.

It is important to note from the above figures that the density values of compacts made from both as-received and milled powder for conventionally-sintered parts are very close to each other. Whereas the variation density values for microwave sintered compacts made from as-received and milled chromium powder is more. Probably there is some difference in the solid phase sintering stage between two heating mode.

### 4.2.3 Hardness of Sintered Specimens

Hardness values of sintered pellets were measured using a Leco LM 300 Microindentation hardness tester and it is shown in Table 4.4. The reported hardness values are an average of five readings. It is remarkable to note that the hardness achieved by microwave sintering is far superior to those of conventional sintering. Higher hardness values in the range of 41-98 Hv were obtained for specimens of all conditions sintered by microwave sintering method as compared to range of 22-74 Hv were observed in conventionally sintered specimen. It is worth noting that for all conditions, microwave sintering results in up to 37 % improvement in hardness. This can be attributed to the higher densification and a more refined microstructure in case of microwave sintered specimen.

**Table 4.4**: Microhardness values (HV 0.5) of compacts with green density values as 57%, 67% and 78% of TD, conventionally and microwave sintered at 1050°C and each soaked for 30 minutes, 60 minutes and 180 minutes.

| **Green Density Value = 57 % of TD** | | | | | | |
|---|---|---|---|---|---|---|
| **Peak Soaking Time (mins)** | **Conventional** | | | **Microwave** | | |
| | **As-received** | **9 Hr milled** | **18 Hr Milled** | **As-received** | **9 Hr milled** | **18 Hr Milled** |
| **30** | 27 | 26 | 30 | 54 | 42 | 43 |
| **60** | 22 | 28 | 29 | 57 | 56 | 47 |
| **180** | 22 | 31 | 29 | 59 | 44 | 41 |
| **Green Density Value = 67 % of TD** | | | | | | |
| **Peak Soaking Time (mins)** | **Conventional** | | | **Microwave** | | |
| | **As-received** | **9 Hr milled** | **18 Hr Milled** | **As-received** | **9 Hr milled** | **18 Hr Milled** |
| **30** | 29 | 35 | 33 | 67 | 63 | 54 |
| **60** | 36 | 46 | 43 | 66 | 61 | 67 |
| **180** | 40 | 41 | 53 | 75 | 65 | 65 |
| **Green Density Value = 78 % of TD** | | | | | | |
| **Peak Soaking Time (mins)** | **Conventional** | | | **Microwave** | | |
| | **As-received** | **9 Hr milled** | **18 Hr Milled** | **As-received** | **9 Hr milled** | **18 Hr Milled** |
| **30** | 53 | 55 | 65 | 75 | 98 | 86 |
| **60** | 51 | 66 | 69 | 68 | 85 | 93 |
| **180** | 55 | 63 | 74 | 76 | 87 | 97 |

As seen from Table 4.3 microwave sintered samples contains comparatively less pores and voids and also less grain growth occurred than conventional specimen. The elimination of pores by coarsening of grains is the main mechanism of sintering by conventional sintering technique whereas in microwave sintering densification of compacts occurs by different mechanism. It is known that microwave interact readily with

high dielectric constant [51]. Thus this leads to elimination of pores without much coarsening of the grains.

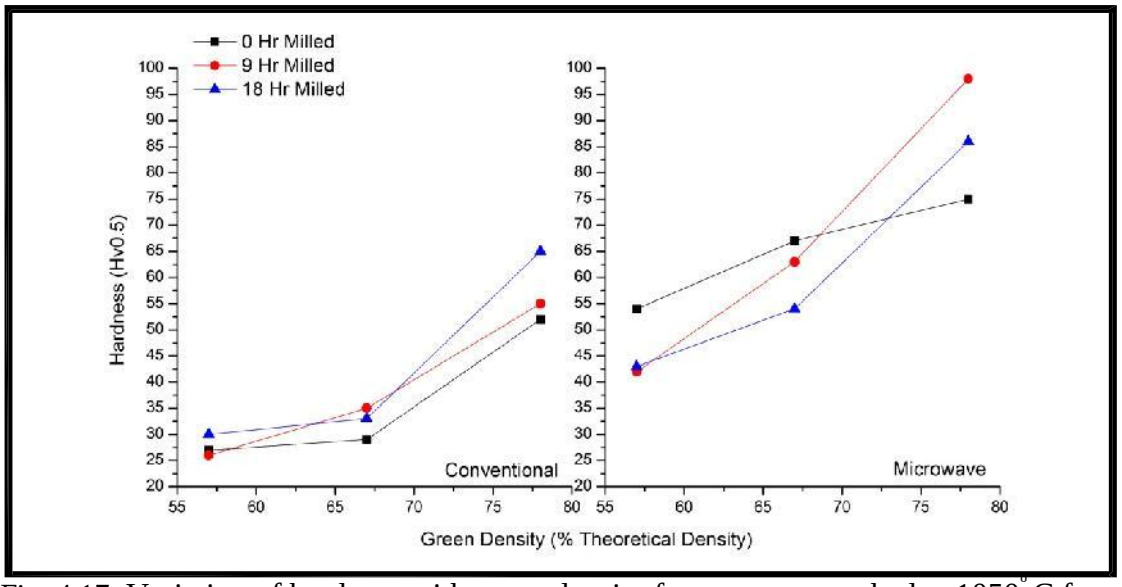


Fig. 4.17: Variation of hardness with green density for compacts soaked at 1050° C for 30 mins in conventional and microwave furnace.

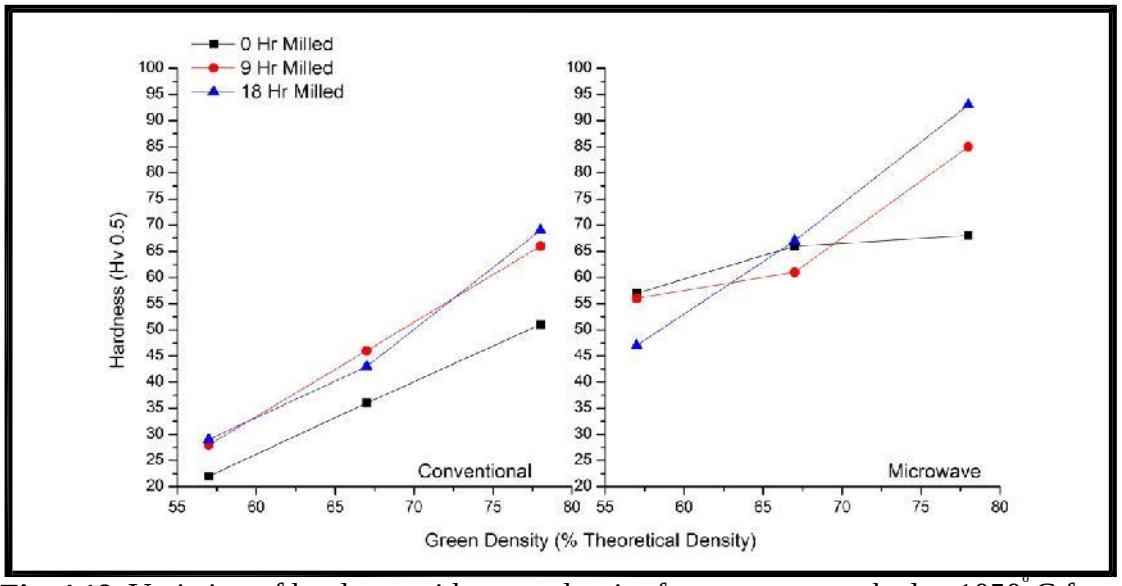


**Fig. 4.18**: Variation of hardness with green density for compacts soaked at 1050° C for 60 mins in conventional and microwave furnace.

Therefore it can be concluded that increase in hardness is a function of presence of Cr and density of sintered specimen. It is clearly evident from the figures 4.17 to 4.19 that hardness increases with the increase in the green density because at higher compaction pressure, more number of interparticle contacts takes place which results in formation of more contiguous structure which further leads to improvement in hardness values.

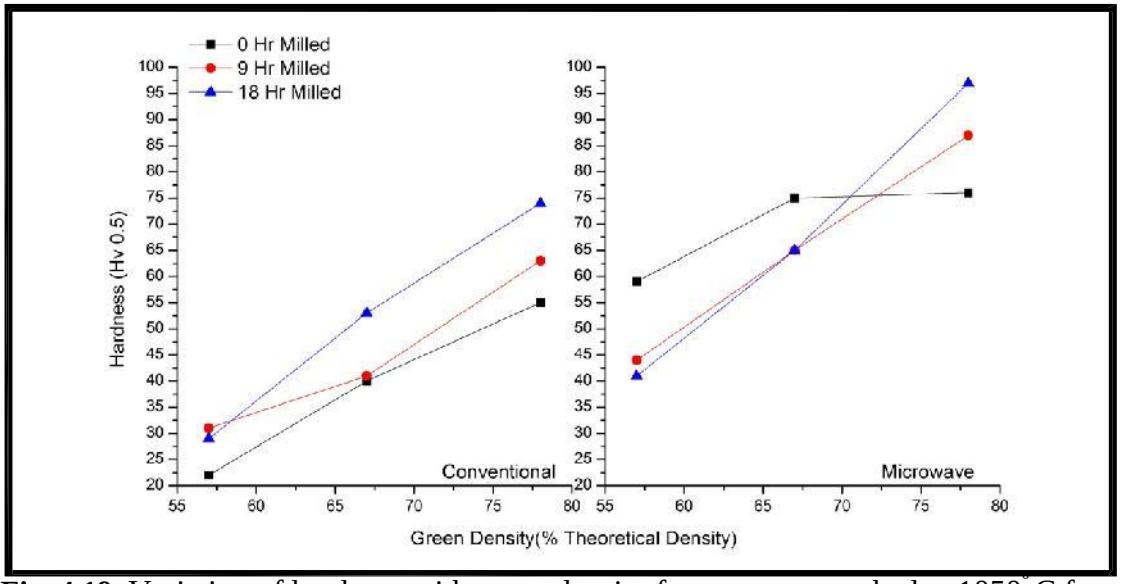


**Fig. 4.19**: Variation of hardness with green density for compacts soaked at 1050° C for 180 mins in conventional and microwave furnace.

Figures 4.20 to 4.22 compare the hardness of conventionally and microwave sintered specimens with three peak soaking times. It seems soaking time exerts limited influence on the hardness value especially for microwave- sintered specimens. With soaking duration increasing from 30 to 180 minutes, hardness values of microwave sintered specimen heighted by 4.4% and 13.3% in case of conventionally sintered specimens.

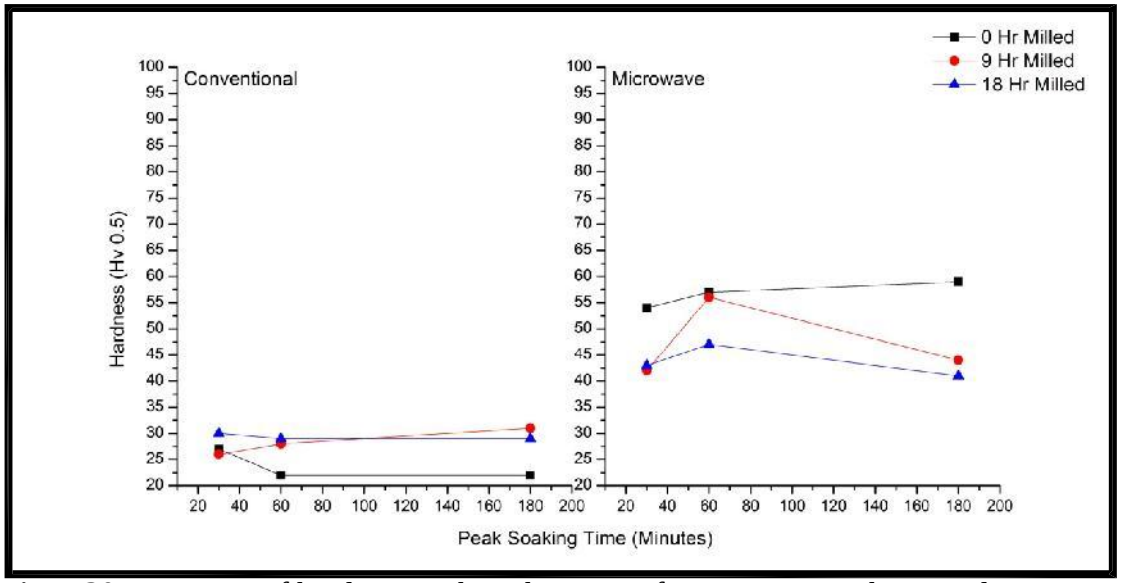


**Fig. 4.20**: Variation of hardness with soaking time for compacts with green density 57% of TD sintered in conventional and microwave furnace.

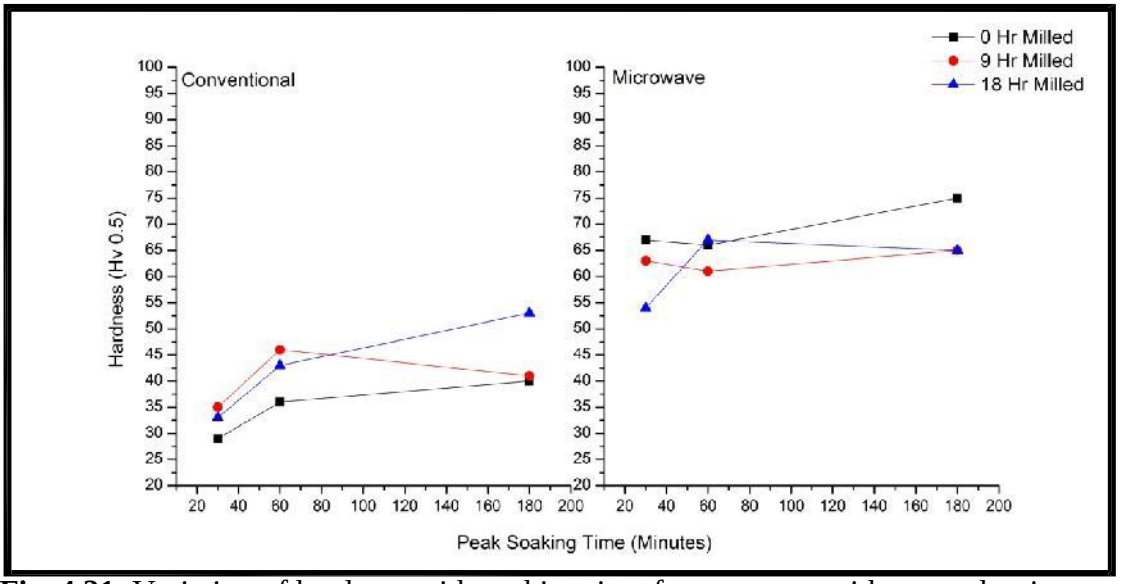


**Fig. 4.21**: Variation of hardness with soaking time for compacts with green density 67% of TD sintered in conventional and microwave furnace.

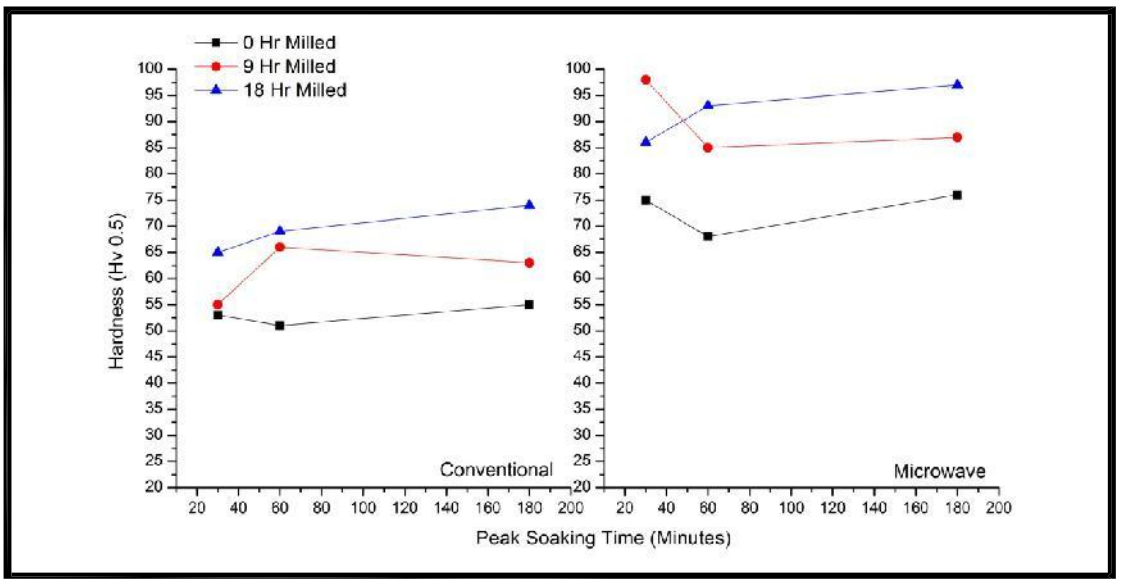


**Fig. 4.22**: Variation of hardness with soaking time for compacts with green density 78% of TD sintered in conventional and microwave furnace.

However, the effect of mechanical milling of Cr powder on hardness of sintered samples is not very distinct especially for microwave sintered specimens.

### 4.2.4 Electrical Conductivity of Sintered Specimens

Electrical conductivity of the sintered specimens of all the conditions sintered by conventional sintering and microwave sintering were measured and compared with the conductivity as per the International Annealed Copper Standard (IACS) (100%) and listed in the Table 4.5 below. The conductivity was measured using 4-probe method in SIGMATEST D 2.068, FOERSTER instrument.

It can be noted from Table 4.5 that electrical conductivity gradually increases when sintering method was changed from conventional to microwave sintering. The overall enhancement in electrical conductivity by using microwave technique is approximately 30 %. It should be mentioned here that improvement in conductivity was calculated by considering the average values of both the technique.

**Table 4.5**: Electrical Conductivity values (% IACS) of compacts with green density values as 57%, 67% and 78% of TD, conventionally and microwave sintered at 1050°C and each soaked for 30, 60 and 180 minutes.

| **Green Density Value = 57 % of TD** | | | | | | |
|---|---|---|---|---|---|---|
| **Peak Soaking Time (mins)** | **Conventional** | | | **Microwave** | | |
| | **As-received** | **9 Hr milled** | **18 Hr Milled** | **As-received** | **9 Hr milled** | **18 Hr Milled** |
| **30** | 15 | 9 | 7 | 28 | 13 | 20 |
| **60** | 14 | 10 | 9 | 18 | 19 | 7 |
| **180** | 14 | 8 | 7 | 17 | 18 | 11 |
| **Green Density Value = 67 % of TD** | | | | | | |
| **Peak Soaking Time (mins)** | **Conventional** | | | **Microwave** | | |
| | **As-received** | **9 Hr milled** | **18 Hr Milled** | **As-received** | **9 Hr milled** | **18 Hr Milled** |
| **30** | 23 | 13 | 12 | 35 | 25 | 25 |
| **60** | 25 | 16 | 13 | 31 | 24 | 25 |
| **180** | 26 | 14 | 12 | 30 | 27 | 27 |
| **Green Density Value = 78 % of TD** | | | | | | |
| **Peak Soaking Time (mins)** | **Conventional** | | | **Microwave** | | |
| | **As-received** | **9 Hr milled** | **18 Hr Milled** | **As-received** | **9 Hr milled** | **18 Hr Milled** |
| **30** | 32 | 25 | 23 | 36 | 34 | 30 |
| **60** | 34 | 26 | 21 | 34 | 24 | 30 |
| **180** | 32 | 26 | 22 | 35 | 38 | 31 |

From the above table, electrical conductivity of the compacts was found to be stronger function green density values and a weaker function of soaking time. When green density was increase i.e. from 57 % to 78 % of TD in case of microwave sintering electrical conductivity found to be higher. This is because for higher green density compacts, a little higher densification was observed by elimination of porosity (Table 4.3) which helps in improving bonding among particles. This make easier to flow electron and achieve higher conductivity [52].

However, with up to 18 hours milling of Cr powder the electrical conductivity values are decreasing significantly for compacts in both the methods. This is expected as because with mechanical milling the contamination of powder, with elements like Fe

and C, has increased where conductivity of such elements is much lower than that of Cu.

Also, after mechanical milling the particle size reduced to finer size. It is know that smaller size particles/crystallite size contributes less electrical conductivity because grain boundaries acts as a centre of electron scattering [53]. This might be significant factor in reduction of electrical conductivity.

The influence of gas content is also considerable. It is certainly that the content of gas and its distribution have an influence on the conductivity [54]. During mechanical milling oxidation of chromium must have increased to a considerable level such that during consolidation gas content increases which results in reduction of electrical conductivity.

## 4.3 Analysis of Parts Designed for Microwave Furnace

The static analysis of two designed assemblies for microwave furnace was performed in order to determine maximum stress and deformation occurring on quartz and calcium fluoride glass under high vacuum i.e. $10^{-5}$ mbar and other operating conditions. The solid models developed using Solidworks were exported to Ansys 11.0 software for further analysis. Figure 4.23 shows the FE model of side window and top window for sintering furnace.

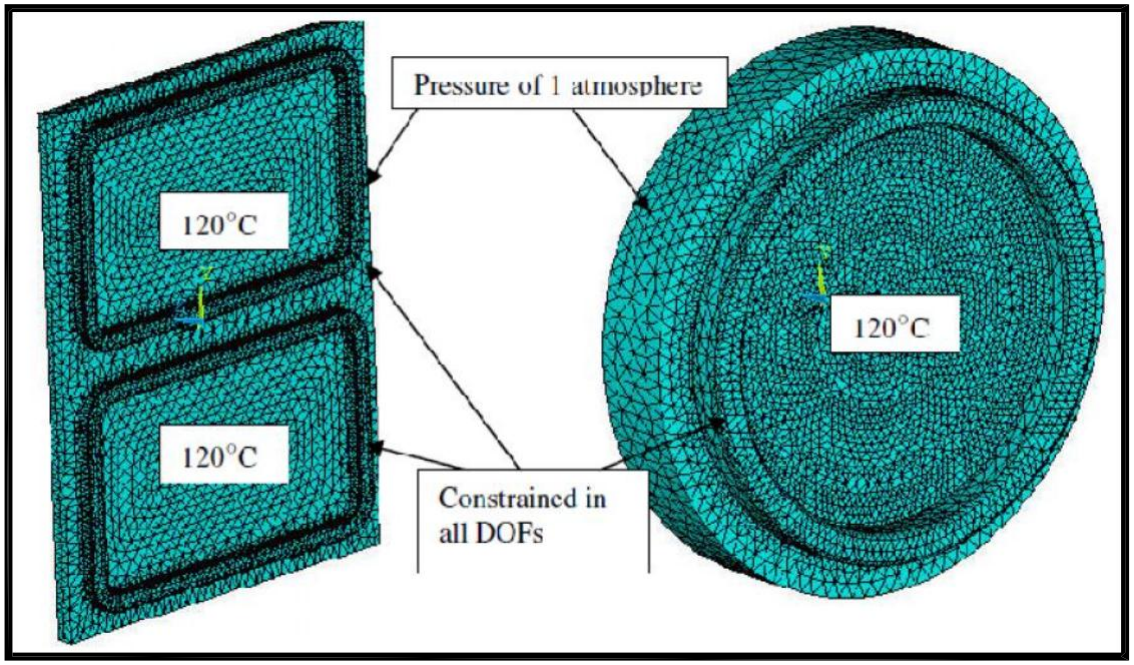


**Fig. 4.23**: FE models of side window glass (left) and top window glass (right).

The analysis was carried out in two stages. In first stage, Thermal analysis was carried out and for second stage nodal solution was used for Structural analysis. Only glass and O-ring were considered for the analysis purpose.

For Thermal Analysis meshing of solid model was done using Solid 87 element. The ambient conditions were assumed to be at 25 $^{\circ}$C and the convective coefficient for interface between quartz glass and atmosphere considered was 10 W/m$^2$K. Temperature of 120 °C was applied on the glass surface which is exposed to inside of furnace and pressure of 1 atmosphere (101325 Pa) was applied on the other surface.

It was also assumed that both the glasses were not constrained in any of the direction because there was a clearance of 1 mm in all directions whereas O-rings were made constrained in all directions.

After completion of Thermal analysis, the nodal solution was imported to Structural analysis. For loading condition, $10^{-6}$ mbar pressure was considered for inside of furnace and 1 atmospheric pressure for outside of furnace.

Under the application of thermal and vacuum loads, maximum deformation in quartz glass was observed to be 0.15 mm as shown in Figure 4.24

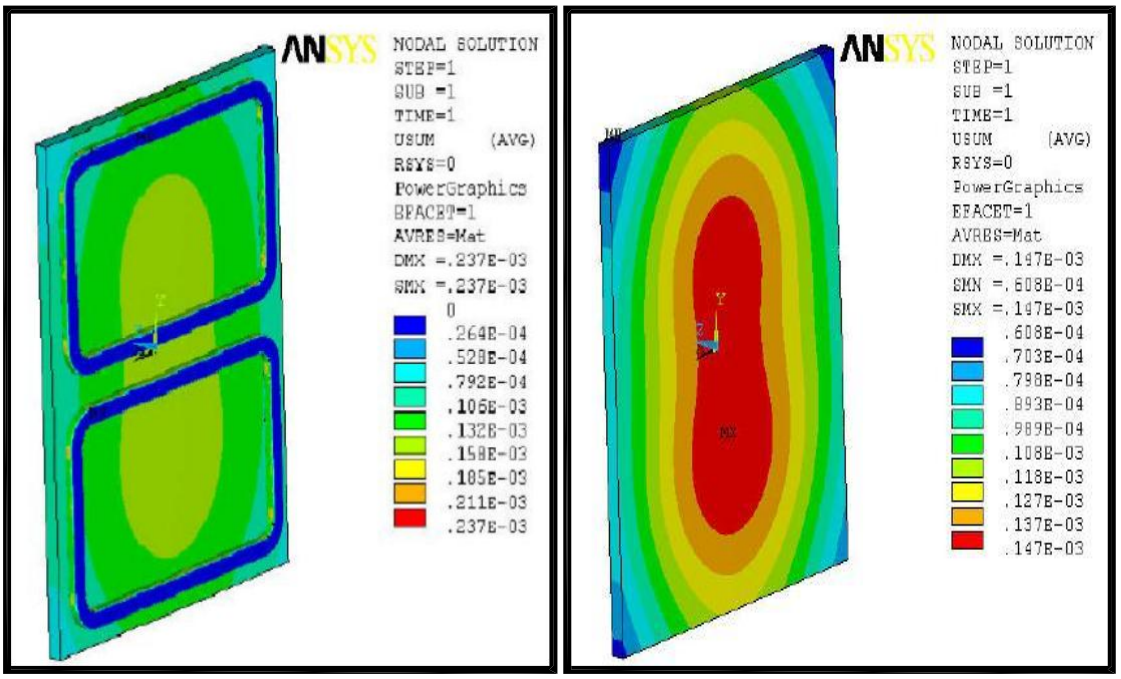


**Fig. 4.24**: Deformation plot on quartz window glass.

Also, maximum stress for quartz glass was observed to be 9.6 MPa which is well within the limit of allowable stress i.e. 48 MPa (Tensile Strenght) as shown in Figure 4.25

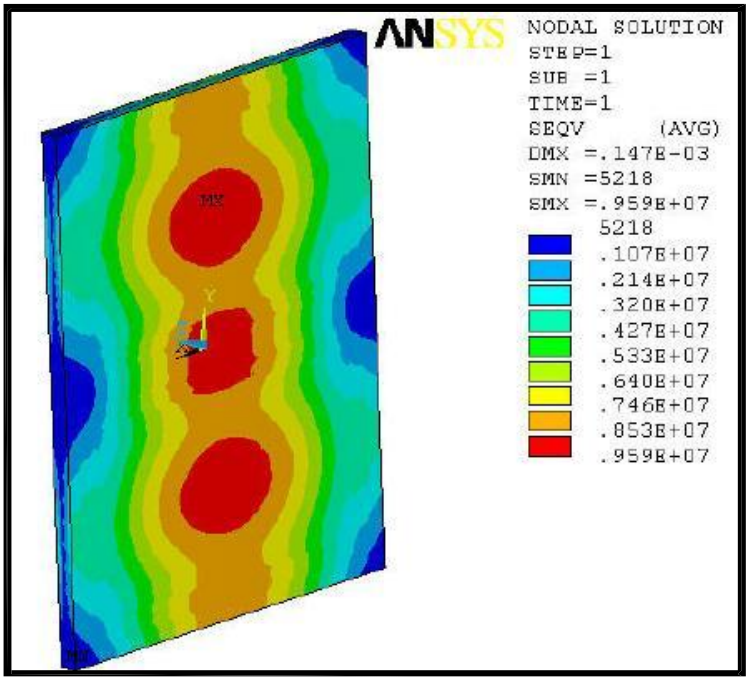


**Fig. 4.25**: Equivalent stress plot on quartz window.

In case of calcium fluoride glass, maximum deformation was observed to be 0.13 as shown in Figure 4.26 and maximum stress was observed to be 0.7 MPa which is very less, shown in Figure 4.27

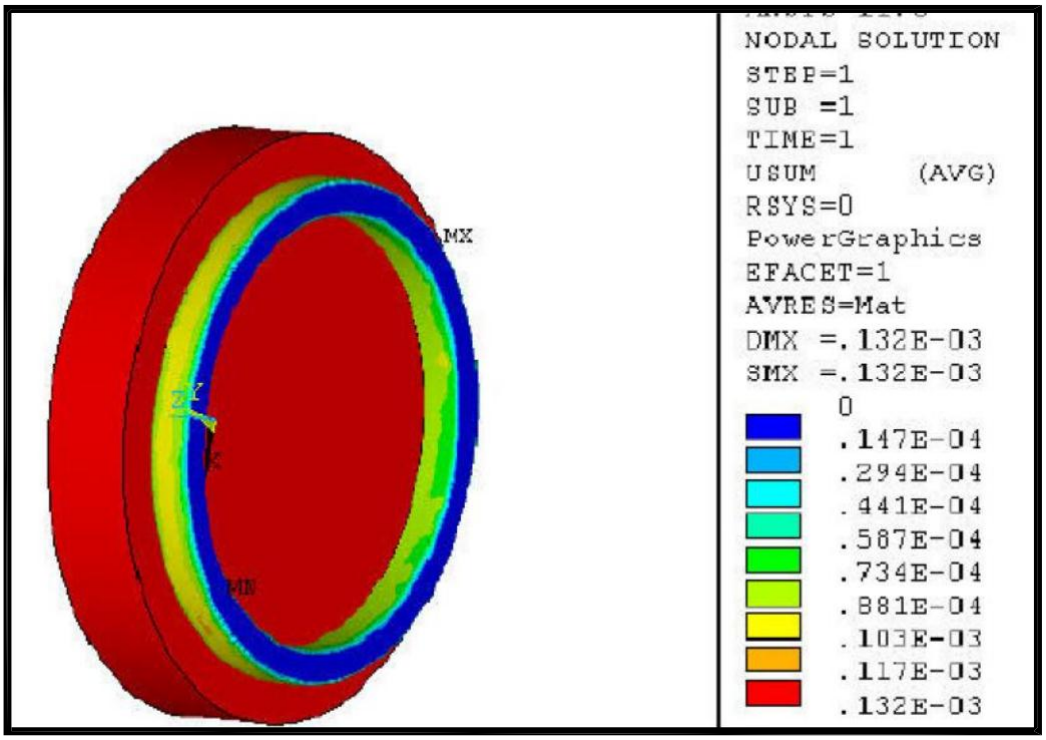


**Fig. 4.26**: Deformation plot on calcium fluoride window glass.

From the above analysis it is clear that both the glasses can be successfully used for microwave furnace under high vacuum condition.

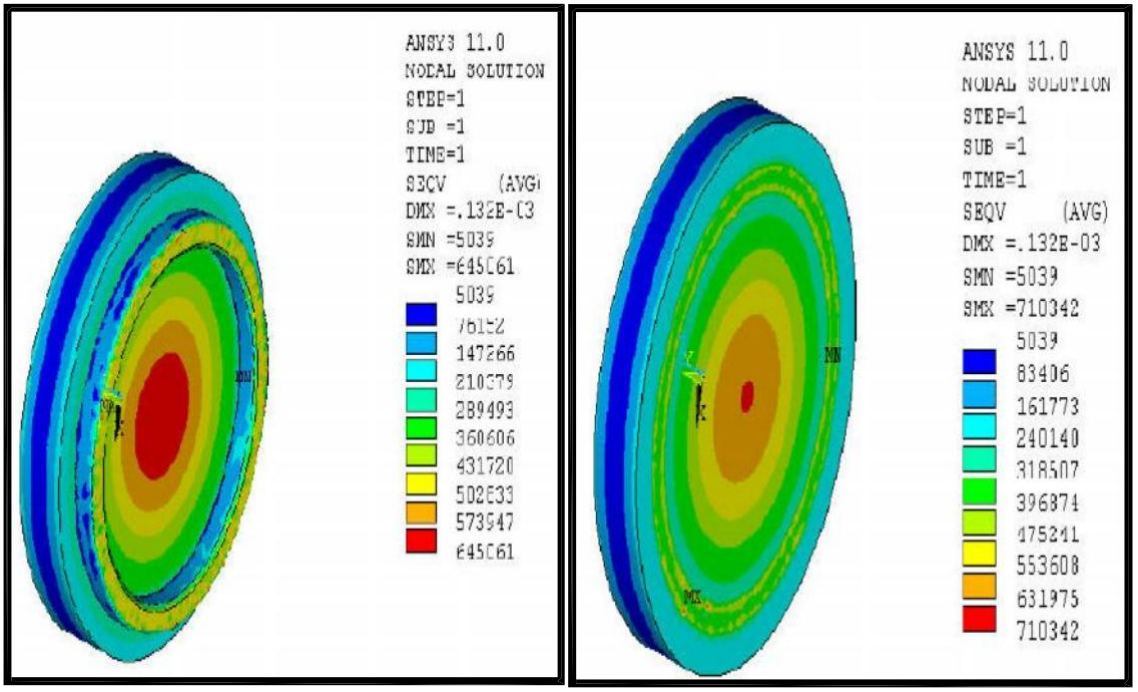


**Fig. 4.27**: Equivalent stress plot on calcium fluoride glass.

# Chapter 5 Conclusion and Future Scope of Study

## 5.1 Conclusion

a) In the present investigation attempts have been made to synthesize Cu-75Cr contact material with as-received Cr powder and milled Cr powder developed by mechanical milling (milled for maximum 18 hours) followed by conventional sintering and microwave sintering methods.

b) XRD, Particle size and BET surface area revealed that maximum crystallite/particle size reduction took place for 9 hour milled powder instead of 18 hour milled powder. Crystallite size and average particle size came out to be 34 nm and ~3µm, respectively.

c) In comparison to conventional sintering method, there is about 75 % reduction in process time during microwave sintering.

d) SEM analysis revealed that microwave sintering produces well rounded and finer chromium particles well separated from each other as opposed to the sharp, irregular and wedge shaped chromium particles for the conventionally-sintered samples. Also, microwave sintering resulted in significantly lower Cr grain coarsening.

e) The maximum densification in conventionally sintered compacts is around 85% of theoretical density whereas sintered compacts by microwave technique shows significantly higher densification, about 92% of theoretical density. The overall enhancement in sintered density by microwave technique is about 6.3% more than conventionally sintered compacts.

f) Higher hardness values in the range of 41-98 Hv were obtained for specimens of all conditions sintered by microwave sintering method as compared to range of 22-74 Hv were observed in conventionally sintered specimen. Microwave sintering results in up to 37 % improvement in hardness.

g) The microwave sintered compacts showed superior electrical conductivity compared to the conventional sintered compacts.

h) Therefore, microwave sintering is found to be most effective in consolidation of Cu-Cr alloy powder compared to the conventional method used in the present investigation as suitable combination of mechanical and electrical properties were obtained using this technique. Therefore the material

developed in the present investigation could be successfully used as contact material for vacuum interrupters.

i) After design modification and its analysis, microwave sintering furnace can be successfully used for its application at $10^{-5}$ mbar pressure.

## 5.2 Future Scope of Study

a) Cu-Cr nanocomposite could be developed by the process of mechanical alloying with varying amount of Cr (5% to 50%) in more intensive grinding media at larger speed.

b) Consolidation could be carried out under high vacuum using both microwave furnace and conventional furnace at varying temperatures e.g. 900 ºC to 1200 ºC to achieve nearest to theoretical density retaining nano-features in the bulk specimens, as increase in the density would improve mechanical as well as electrical conductivity.

c) Detail study of effect of mechanical milling on properties is to be carried out all sintered specimens.

# References


1. M.A. Morris and D.G. Morris**, "**Microstructures and Mechanical Properties of Rapidly Solidified Cu-Cr Alloys", *Acta Metallurgia*, v. 35, n.10, 1987, pp. 2511-2522.

2. B. Miao, Y. Zhang, and G. Liu, "Current Status and Developing Trends in Cu-Cr Contact Materials for VCB," *International Symposium on Discharges and Electrical Insulation in Vacuum*, 2004, v. 2, pp. 311-314.

3. R. Roy, D.K. Agrawal, J.P. Cheng, and S. Gedevanishvili, "Full Sintering of Powdered Metals Using Microwaves," *Nature*, v.399, n.17, 1999, pp. 668-670.

4. R.W. Sorensen and H.E. Mendenhall, "Vacuum Switching Experiments at California Institute of Technology", *Trans. AIEE*, v.45, 1926, pp.1102-1105.

5. P.G. Slade, The Vacuum Interrupter: Theory, Design, and Application, CRC Press, 2008.

6. J.D. Cobine, *Trans. A.I.E.E (Communication and Electronics)*, v. 82, 1963, pp.240.

7. A.S. Jogelkar, *Journal of I.E.E (India*), v. 53, 1974, pp. 245.

8. W.J. Boettinger, S.R. Coriell., "Solidification Microstructures: Recent Developments, Future Directions", *Acta Materillia*, 2000, v. 48, pp. 43-70.

9. P. Barkan, J.M Lafferty, T.H. Lee, J.L. Talento, "Development of Contact Materials for Vacuum Interrupters", *IEEE*, v. 90, 1971, pp. 350.

10. P.G. Slade, "Advances in Material Development for High Power Vacuum Interrupter Contacts", *IEEE. Transactions on Components, Packaging and Manufacturing Technology -Part A*, v. 17, 1994, pp. 276-289.

11. T. B. Massalski, Binary Alloy Phase Diagrams Vol. 2, pp. 1266-1268, ASM International, 1990

12. A.A. Robinson, "Vacuum Type Electric Circuit Interrupting Devices", British patent No. 1194674, 1970

13. H. Kippenberg, W. Kuhl and W. Schlenk, "Kontaktmaterial fur Vakuumschalter", *Siemens Energie u. Automation*, v. 7, 1985, pp. 18-21.

14. R. Muller, "Arc-Melted CuCr Alloy Contact Materials for Vacuum Interrupters", *Siemens Forsch. u. Entwickl.*,v. 3, 1988, pp.105-111.

15. H. Schellekans, W. Shang, K. Lenstra, "Plasma sprayed contact materials for vacuum interrupters", *IEEE Transaction on Plasma Science*, 1993.

16. W. F. Rieder, M. Schussek, W. Glatzle, And E. Kny, "The Influence of Composition and Cr Particle Size of Cu/Cr Contacts on Chopping Current, Contact Resistance, and Breakdown Voltage in Vacuum Interrupter", *IEEE Transactions On Components, Hybrids, And Manufacturing Technology*, v. 12, 1989.

17. Y. Wang and B. Ding, "The Preparation And The Properties Of Microcrystalline And Nanocrystalline Cucr Contact Materials", *IEEE Transcation on Components and Packaging Technology*, v. 22, 1999, pp. 467-472.

18. W. Yongxing, Z. Jiyan, C. Jiyuan, W. Yi, W. Xiumin, "Investigation on the Properties of CuCr Contact Material after Cryogenic Treatment", *IEEE*, 2006, pp.38-41.

19. H. Fink, D. Gentsch and M. Heimbach, "Multilayer Contact Material Based on Copper and Chromium and Its Interruption Ability", *IEEE Transaction on plasma science*, v. 31, 2003, pp. 973-976.

20. I. Lahiri and S. Bhargava, "Compaction and Sintering Response of Mechanically Alloyed Cu-Cr Powder", *Powder Technology*, v.189, 2009, pp. 433-438.

21. R.M. Davis, B. McDermott, and C.C. Koch, "Mechanical Alloying of Brittle Materials", *Metall. Trans. A*, v.19, 1988, pp. 2867–74.

22. B.Q. Han, D. Matejczyk, F. Zhou, Z. Zhang, C. Bampton, E.J. Lavernia and F.A. Mohamed, "Mechanical Behavior of a Cryomilled Nanostructured Al-7.5%Mg Alloy", *Metallurgical and Materials Transactions A*, v.35, 2004, pp. 947-949.

23. F. Zhou, D. Witkin, S.R. Nutt and E.J. Lavernia, "Formation of Nanostructure in Al Produced by a Low-energy Ball Milling at Cryogenic Temperature, "*Materials Science Engineering A*, vols. 375- 377, 2004, pp. 917-921.

24. J.S. Benjamin, "New Materials by Mechanical Alloying Techniques", *DGM Informations Gesellschaft*, 1998, pp. 3-18.

25. C.C. Koch, O.B. Cavin,C.G. McKamey, J.O. Scarbrough, *Applied Physics Letter*, v. 43,1983, pp.1017-19.

26. A.E. Ermakov, E.E Yurchikov, V.A. Barinov, *Physical Metallurgy Metallography*, v.52, 1981, pp.50-58.

27. C.C. Koch, "Processing of Metals and Alloys", *Materials Science and Technology, Weinheim, Germany: VCH Verlagsgesellschaft Gmbh*, v.15, 1991, p. 193-245.

28. ASM Metals Handbook Vol. 7: Powder Metal Technologies and Applications, ASM International, 1998.

29. M.O. Lai, L. Lu, Mechanical Alloying, Kluwer Academic Publishers, 1998.

30. J. Cheng, R. Roy and D. Agrawal,"Experimental Proof of Major Role of Magnetic Field Losses In Microwave Heating of Metal And Metallic Composites*," Journal of Materials. Science. Letter*, v.20, pp. 1561-1571.

31. P. Yadoji, R. Peelamedu, D. Agrawal, and R. Roy, "Microwave Sintering of Ni-Zn Ferrite: Comparison with Conventional Sintering," *Material Science & Engineering*, 2003, pp. 269-278.

32. M. Oghbaei, O. Mirzaee, "Microwave Versus Conventional Sintering: A Review of Fundamentals, Advantages and Applications", *Journal of Alloys and Compounds*, v. 494, 2010, pp. 175–189.

33. D.E. Clark, D.C. Folz and J.K. West, "Processing Materials with Microwave Energy," *J. of Materials Science and Engineering*, v. A287, 2000, pp. 153-58.

34. W.H. Sutton, "Microwave Processing of Ceramic Materials", *American Ceramic Society Bulletin*, v. 68, 1989, pp. 376-386.

35. R.J Meredith, Engineers' Handbook of industrial Microwave Heating, IEE, 1998.

36. C. Leonelli, P. Veronesi, L. Denti, A. Gatto, L. Iuliano, *Journal of Materials Processing Technology*, v. 205, 2008, pp. 489–496.

37. S.S. Panda, V. Singh, A. Upadhyaya and D. Agrawal**,** "Sintering Response of Austenitic (316L) and Ferritic (434L) Stainless Steel Consolidated in Conventional and Microwave furnaces", *Scripta Materialia,* v.54, 2006, pp. 2179–2183.

38. D. Agrawal, *Sohn International Symposium Advanced Processing of Metals and Materials*, v. 4, 2006, pp. 183–192.

39. R.R. Menezes, R.H.G.A. Kiminami, *Journal of Materials Processing Technology*, v.203, 2008, pp. 513–517.

40. J.H. Yang, K.W. Song, Y.W. Lee, J.H. Kim, K.W. Kang, K.S. Kim, Y.H. Jung, *Journal of Nuclear Materials*, v. 325, 2004, 210–216.

41. Z.Z. Fang, Sintering Of Advanced Materials: Fundamentals and Processes, Woodhead Publishing Limited, 2010.

42. J. Cheng, D. Agrawal, Y. Zhang, R. Roy, *Materials Letters.* v. 56, 2002, pp. 587–592.

43. J. P. Binner, B. Vaidhyanathan and T. Carney, *Advanced Science Technology*, v. 45 ,2006, pp.835–844.

44. D. K. Agrawal, R. Raghavendra and B. Vaidhyanathan: US patent no. 6399012, 2002.

45. G. Prabhu, A. Chakraborty, B. Sarma, *International Journal of Refractory Metals & Hard Materials*, v. 27, 2009, pp. 545–548.

46. A. Mondal, D. Agrawal, A. Upadhyaya, "Microwave Heating of Pure Copper Powder with Varying Particle Size and Porosity", *Journal of Microwave Power & Electromagnetic Energy*, v. 43, 2009.

47. D.G Kim, G.S. Kim, M.J. Suk, S.T. Oh, Y.D. Kim, *Scripta Mater*. , v. 51, 2004 pp. 677.

48. Z.Q. Yang, C.C. Jia, L. Gan, J. Zhao, Z.Z. Xie, *J. Univ. Sci. Technol. Beijing*, v.24, 2002, pp. 115

49. A. Mondal, A. Upadhyaya, D. Agarwal, "Microwave and Conventional Sintering of 90W-7Ni-3Cu Alloys with Premixed and Prealloyed Binder Phase, *Materials Science and Engineering*, v. A 527, 2010, pp. 6870-6878.

50. Shu-Dong Luo, Jian-Hong Yi, Ying-Li Guo, Yuan-Dong Peng, "Microwave Sintering W-Cu composites": Analyses of Densification and Microstructural Homogenization", *Journal of alloys and compounds*, v. 473, 2009.

51. G.C. Reddy GC, K. Rajkumar, S. Aravindan, *International Journal of Advanced Manufacturing Techology*, v.48, 2010, pp. 645.

52. V. Rajkovic, D. Bozic, M.T Jovanovic, Journal of Alloy and compound, v. 459, 2008 p. 177.

53. B.S. Murty, T. Venugopal, K.P Rao, *Acta Metallurgia*, v. 55, 2007, pp. 4439.

54. J.He, T.Matsumura, "3-Dimensional Simulation on Electrical Conductivity of CuCr Contact Materials", *Trans. IEE of Japan*, v.121-B, n.8, 2001, pp.924-929.